

# Bayesian Dynamic Fused LASSO

Kaoru Irie\*

May 30, 2019

## Abstract

The new class of Markov processes is proposed to realize the flexible shrinkage effects for the dynamic models. The transition density of the new process consists of two penalty functions, similar to Bayesian fused LASSO in its functional form, that shrink the current state variable to its previous value and zero. The normalizing constant of the density, which is not ignorable in the posterior computation, is shown to be essentially the log-geometric mixture of double-exponential densities and treated as a part of the likelihood. The dynamic regression models with this new process used as a prior is conditionally Gaussian and linear in state variables, for which the posterior can be computed efficiently by utilizing the forward filtering and backward sampling in Gibbs sampler. The latent integer-valued parameter of the log-geometric distribution is understood as the amount of shrinkage to zero realized in the posterior and can be used to detect in which period the corresponding predictor becomes inactive. With the hyperparameters and observational variance estimated in Gibbs sampler, the new prior is compared with the standard double-exponential prior in the estimation of and prediction by the dynamic linear models for illustration. It is also applied to the time-varying vector autoregressive models for the US macroeconomic data and performs as an alternative of the dynamic model of variable selection type, such as the latent threshold models.

*Key words and phrases:* Dynamic shrinkage, fused LASSO, dynamic linear models, forward filtering and backward sampling, scale mixture of normals, synthetic likelihoods.

## 1 Introduction

The univariate dynamic linear models (DLMs) in practice are frequently over-parametrized because of the massive amount of predictors, most of which are believed to be noises. For example, the time-varying vector autoregressive models are typically decomposed into the multiple univariate sub-models for the computational feasibility (e.g., Zhao et al. 2016 and Gruber and West 2016), but this approach results in the excess amount of predictors in those sub-models even for the moderate dimensional observations. This research contributes to the appropriate modeling of sparsity in the univariate DLMs with many predictors by defining a new shrinkage prior on the dynamic coefficients, and its application to the modeling of multivariate time series.

Specifically, for the univariate state variable  $x_t$ , which is the time-varying regression coefficient in the context of DLMs, we consider the new Markov process defined by its transition density,

$$p(x_t|x_{t-1}) \propto \exp \{ -a|x_t| - b|x_t - x_{t-1}| \} \quad (1)$$

---

\*Assistant Professor of Economics, The University of Tokyo. This research was supported in part by Grant-in-Aid for Scientific Research from Japan Society for the Promotion of Science (17K17659).

The two penalty functions in the exponential realize the conditional shrinkage effects. By using this process as the prior in DLMS, we shrink the state variable at time  $t$  toward zero by the first penalty function, while shrinking it to the previous state variable at  $t-1$  as well to penalize the excess dynamics by the second penalty. The technical difficulty is apparently the unknown normalizing constant abbreviated in equation (1) that involves state variable  $x_{t-1}$  and is not ignorable in the posterior analysis. The objective of this research is to compute this normalizing constant explicitly and provide the computational methodology for the efficient posterior analysis by Markov chain Monte Carlo methods.

The prior in (1) is named *dynamic fused LASSO* (DFL) prior for its similarity to Bayesian fused LASSO models (e.g., Kyung et al. 2010 and Betancourt et al. 2017). The Bayesian fused LASSO has rarely been applied to the time series analysis and the problem of unknown normalizing constant has not been discussed. This is because, in Bayesian fused LASSO, the state variables are modeled *jointly*, not conditionally, by exponentiating the various penalty functions to define the joint density of all the state variables. By modeling the joint density directly, the normalizing constant becomes free from the state variables, which simplifies the Bayesian inference for the fused LASSO models and enables the scale mixture representation of the double exponential priors, as in the standard Bayesian LASSO models (Park and Casella, 2008). From this viewpoint, our research is clearly different from the existing fused LASSO models in modeling the *conditional* distribution of state variables to realize our prior belief in the dynamic modeling, which instead poses the problem of computing the normalizing constant that has been ignored (or not required to compute) in the study of the Bayesian fused LASSO. The modeling of the conditional distribution is crucial in predictive analysis; the direct application of the existing fused LASSO to the joint distribution of time-varying parameters does not define the conditional distribution coherently, and cannot be used for sequential posterior updating and forecasting.

Although the normalizing constant complicates the prior and posterior distributions of the DLMS with the DFL process, we prove the augmented model representation of the DFL prior as the conditionally dynamic linear models (CDLMS), for which the efficient posterior sampling of state variables by the forward filtering and backward sampling (FFBS, e.g., see West and Harrison 1997) is available. Facilitating the posterior computation by FFBS with the help of the CDLM representation is the standard strategy in the literature of econometrics and forecasting, where the dynamic sparsity has been realized by the hierarchical DLMS (e.g., Frühwirth-Schnatter and Wagner 2010, Belmonte et al. 2014 and Bitto and Frühwirth-Schnatter 2019). This hierarchical version of dynamic linear models is obtained by the natural extension of DLMS with another prior on its scale parameters in the state equation. While the posterior of state variables is easily computed by FFBS, these priors penalize only the distance between the two consecutive state variables,  $x_t$  and  $x_{t-1}$ , which is understood as the special case of the prior of this study with  $a = 0$  in equation (1). Our approach, in contrast, integrates the additional penalty for the shrinkage toward zero explicitly into the conditional distribution of the prior process. This modeling approach reflects our prior belief that the state variable is likely to be either zero or unchanged from its previous value. The additional shrinkage effect to zero in the DFL prior can also address the problem of the shrinkage effect restricted to be uniform over time, as pointed out by Uribe and Lopes (2017) as “horizontal shrinkage”, by localizing the shrinkage effect at each time by customized latent parameters, in a different way to Kalli and Griffin (2014), Uribe and Lopes (2017) and Kowal et al. (2019).

The conditional normality and linearity of the DFL prior is based on the fact that the prior process is decomposed into two parts: the synthetic likelihood and synthetic prior. These terminologies literally mean that the prior consists of two components, one of which is treated as (part of) likelihood and the other of which serves as the prior. The synthetic prior is just the well-known scale mixture of Gaussian autoregressive process, hence normal and linear in state variables. The synthetic likelihood part is equivalent to observing the artificial data  $z_t = 0$  with mean  $x_t$  that provides the additional information to shrink the state variable to zero. The posterior of this CDLM is equivalent to that of the original model,

which justifies the use of FFBS for the model with the synthetic likelihood. The idea of synthetic likelihood and prior approach has been utilized for the study of optimal portfolios that are sparse and less switching (e.g., Kolm and Ritter 2015 and Irie and West 2019), and this research consider the same idea in the context of statistical modeling.

The conditional density and its unknown normalizing constant are analyzed via the well-known scale mixture representation of the double exponential distributions (Andrews and Mallows 1974 and West 1987), which has been applied to the Bayesian LASSO models. A methodological alternative is the approach of Hans (2009, 2011) to the Bayesian LASSO and elastic net models in which the conditional posterior density becomes the mixture of truncated normals. While this approach is efficient in computation by avoiding any continuous latent parameters being newly introduced, the scale mixture approach is useful in analytically computing the DFL process in a simple way. By taking the scale-mixture approach, we find that the normalizing constant translates as the synthetic likelihoods, enabling for the straightforward implementation of Gibbs sampler. The truncated distributions in the high-dimensional parameter space are computationally costly and should be avoided, which also motivates the scale-mixture approach.

The rest of the paper is structured as follows. Section 2 introduces the class of the new Markov processes in the general form, including the DFL process as its special case. Section 3 focuses on the DFL prior in (1) and proves its CDLM representation that helps understanding the implied prior belief about shrinkage effects in this model. Section 4 provides the MCMC algorithm for the DLMS with the DFL prior by using the properties proven in the previous sections, in addition to discussing the estimation of hyperparameters and observational variances. In Section 5, the proposed model is applied to the simulation data for illustration (Section 5.1) and to the US macroeconomic time series for the comparison with the model of the variable selection type (Section 5.2). The paper is concluded in Section 6 with the potential future research.

**Notations:** The density of the univariate normal distribution with mean  $\mu$  and variance  $\sigma^2$  evaluated at  $x$  is denoted by  $N(x|\mu, \sigma^2)$ . The double-exponential density with parameter  $a$  is denoted by  $DE(x|a) = (a/2)e^{-a|x|}$ . The gamma distribution with shape  $\alpha$  and rate  $\beta$  is written as  $Ga(\alpha, \beta)$  with mean  $\alpha/\beta$ . The generalized inverse Gaussian distribution is denoted by  $GIG(p, \alpha, \beta)$ , the density of which is proportional to  $x^{p-1} \exp\{-(\alpha x + \beta/x)/2\}$ .

## 2 A new Markov process

### 2.1 General form of the process

A new class of univariate Markov processes  $\{x_t\}_{t=1,2,\dots}$  is defined by its conditional density of transition  $p(x_t|x_{t-1})$  or, equivalently, the loss function tied to the density by  $L(x_t|x_{t-1}) = -\log p(x_t|x_{t-1})$ , ignoring the constant. This transformation of probabilistic models to loss functions has been studied for statistical analysis and decision making problems (e.g., see Müller, 1999). The loss functions proposed in this research consist of two penalty terms in the additive form as  $L_1(x_t) + L_2(x_t - x_{t-1})$ , where functions  $L_i(\cdot)$  for  $i = 1, 2$  satisfy  $L_i(x) = L_i(-x) \geq 0$  for any real  $x$ . The exponential transformation of this loss function defines the conditional probability density,

$$p(x_t|x_{t-1}) \propto \exp\{-L_1(x_t) - L_2(x_t - x_{t-1})\} \quad (2)$$

This study focuses on the special case of this class of models that defines the loss functions by  $L_1(x) = a|x|$  and  $L_2(x) = b|x|$  for some nonnegative weights  $a, b > 0$ , which implies the process in equation (1). The two different types of shrinkage effects are clearly seen in this functional form; one is the shrinkage of  $x_t$

to the previous point  $x_{t-1}$  and the other to zero. It is important to note that the normalizing constant, which is abbreviated in (2), does depend on  $x_{t-1}$ , which complicates the joint density of  $x_{1:T}$ .

The exponentiated loss functions are assumed to be integrable. Equivalently, they are proportional to some probability density functions denoted by

$$f(x_t) \propto \exp\{-L_1(x_t)\}, \quad \text{and} \quad g(x_t, x_{t-1}) \propto \exp\{-L_2(x_t - x_{t-1})\}$$

where  $f(x)$  and  $g(x, x')$  are probability density functions of  $x$ . Also,  $g(x, x')$  is assumed to be symmetric;  $g(x, x') = g(x', x)$  for any pair  $(x, x')$ , by definition. Also, the normalizing constant of  $g$  density is independent of  $x'$ , i.e., the integral of  $g(x, x')$  in  $x$  does not depend on  $x'$ . The process in equation (2) is written as

$$p(x_t|x_{t-1}) = \frac{f(x_t)g(x_t, x_{t-1})}{h(x_{t-1})}, \quad \text{where} \quad h(x') = \int_{-\infty}^{\infty} f(x)g(x, x')dx \quad (3)$$

The analytical expression of  $h(x_{t-1})$  for the  $\ell_1$  loss functions is discussed later in Proposition 3.1.

Denote the marginal distribution of  $x_t$  by  $\pi(x_t)$ . The condition for this process to be stationary is

$$\pi(x_t) = \int_{-\infty}^{\infty} \frac{f(x_t)g(x_t, x_{t-1})}{h(x_{t-1})} \pi(x_{t-1}) dx_{t-1}$$

and one solution of this functional equation is  $\pi(x) = h(x)f(x)$ , with which the process also becomes reversible. In the following, we assume the stationarity and the marginal density of this form.

Furthermore, assume that  $f(x)$  and  $g(x, x')$  are the scale mixture of normals,

$$f(x) = \int_0^{\infty} N(x|0, \tau_1) p_1(\tau_1) d\tau_1, \quad \text{and} \quad g(x, x') = \int_0^{\infty} N(x|x', \tau_2) p_2(\tau_2) d\tau_2,$$

for some densities  $p_1$  and  $p_2$ . Many statistical models, that include double-exponential, horseshoe and other distributions, fall in this class of loss functions  $L_i(x)$ , or densities  $f$  and  $g$ . Using this scale-mixture representation, we have

$$f(x)g(x, x') = \int_0^{\infty} \int_0^{\infty} N\left(x \left| \frac{\tau_1}{\tau_1 + \tau_2} x', \frac{\tau_1 \tau_2}{\tau_1 + \tau_2} \right.\right) N(x'|0, \tau_1 + \tau_2) p_1(\tau_1) p_2(\tau_2) d\tau_1 d\tau_2$$

hence the normalizing function  $h(x')$  is

$$h(x') = \int_0^{\infty} \int_0^{\infty} N(x'|0, \tau_1 + \tau_2) p_1(\tau_1) p_2(\tau_2) d\tau_1 d\tau_2 \quad (4)$$

i.e., the scale mixture of normals with the convolution of  $p_1(\tau_1)$  and  $p_2(\tau_2)$ . The conditional density also has the following mixture representation,

$$p(x|x') = \int_0^{\infty} \int_0^{\infty} N\left(x \left| \frac{\tau_1}{\tau_1 + \tau_2} x', \frac{\tau_1 \tau_2}{\tau_1 + \tau_2} \right.\right) \frac{N(x'|0, \tau_1 + \tau_2) p_1(\tau_1) p_2(\tau_2)}{h(x')} d\tau_1 d\tau_2 \quad (5)$$

i.e., the location-scale mixture of normals. Note that the integrand, the normal density of  $x$ , is the regression of  $x$  on  $x'$  with coefficient  $\tau_1/(\tau_1 + \tau_2)$ . Conditioned by the latest state  $x'$ , the current state  $x$  is shrunk toward  $x'$ . The amount of this conditional shrinkage is determined by the balance of two conflicting loss functions,  $L_1$  and  $L_2$ .

## 2.2 Joint distribution and examples

Consider a Markov process  $\{x_t\}_{t=1,2,\dots}$  whose transition  $p(x_t|x_{t-1})$  is given in equation (3) with the initial distribution  $\pi(x_1)$ . The joint distribution of  $x_{1:T}$  can be decomposed into two parts– the synthetic likelihood and prior– as

$$p(x_{1:T}) = \pi(x_1) \prod_{t=2}^T p(x_t|x_{t-1}) = \underbrace{\left\{ \frac{\pi(x_1)}{f(x_1)} \prod_{t=2}^T \frac{f(x_t)}{h(x_{t-1})} \right\}}_{\text{“likelihood”}} \underbrace{\left\{ f(x_1) \prod_{t=2}^T g(x_t, x_{t-1}) \right\}}_{\text{“prior”}}$$

If one ignores the “likelihood” above, the transition simply comprises  $g(x_t, x_{t-1})$ , where the explicit shrinkage of  $x_t$  is set only toward a single point  $x_{t-1}$ , not toward both  $x_{t-1}$  and zero. The Markov process with such a “prior” is widely used in the state space modeling, for the assumption that  $g(x, x')$  has the mixture representation simplifies the posterior computation. The “likelihood” involves the reciprocal of  $h(x_{t-1})$  and feeds the synthetic prior. Hence, the proposed Markov process is characterized as the “posterior” of this synthetic model.

*Example 1:* Gaussian random walk  $x_t|x_{t-1} \sim N(x_{t-1}, \sigma^2)$  is obtained by  $L_1(x) = 0$  and  $L_2(x - x') = (x - x')^2/2\sigma^2$ . Gaussian AR(1) process  $x_t|x_{t-1} \sim N(\phi x_{t-1}, \sigma^2)$  for  $\phi \in (-1, 1)$  is realized by  $L_1(x) = ax^2/2$  and  $L_2(x - x') = b(x - x')^2/2$ , where  $\phi = b/(a + b)$  and  $\sigma^2 = 1/(a + b)$ . These two processes are the typical examples of the prior in DLMs.

*Example 2:* Bayesian elastic net  $L_1(x) = ax^2$  and  $L_2(x - x') = (1 - a)|x - x'|$ . This process is considered in Hans (2011) as the prior of static linear models without the use of scale mixture representation.

*Example 3:* DFL, or the two  $\ell_1$  penalties:  $L_1(x) = a|x|$  and  $L_2(x - x') = b|x - x'|$ . The focus of this research is on the process of this type. In the probability representation,  $f(x) = DE(x|a)$  and  $g(x, x') = DE(x - x'|b)$ , both of which are the scale mixture of Example 1, where the scale parameter follows the gamma distribution with shape 1 and rate  $a^2/2$  or  $b^2/2$ . We refer this model as dynamic fused LASSO, or DFL prior/process. If  $a = 0$ , the model is greatly simplified and easily applied to state space modeling as the dynamic extension of Bayesian LASSO.

*Example 4:* The horseshoe prior (Carvalho et al. 2009, 2010) can be used in modeling this process. The density involves the upper incomplete gamma functions as  $g(x, x') = e^{b(x-x')^2/2}\Gamma(0, b(x-x')^2/2)$ . The horseshoe prior is also the scale mixture of normals; now the scale follows the half-Cauchy distribution (Gelman 2006) or, equivalently, the gamma mixture of gamma distributions. If  $L_1(x) \equiv 0$ , the posterior computation is straightforward. The further extension can be considered as the gamma mixture with the general shape parameters, known as Bayesian bridge models (Polson et al., 2014).

### 3 Dynamic fused LASSO

#### 3.1 Double-exponential models

In the rest of the paper, we focus on the DLF prior of Example 3 in Section 2.2, where the loss functions are  $L_1(x) = a|x|$  and  $L_2(x - x') = b|x - x'|$ . These loss functions imply the double-exponential densities,

$$f(x) = \frac{a}{2}e^{-a|x|} = \int_0^\infty N(x|0, \tau_1)Ga(\tau_1|1, a^2/2)d\tau_1,$$

$$g(x, x') = \frac{b}{2}e^{-b|x-x'|} = \int_0^\infty N(x|x', \tau_2)Ga(\tau_2|1, b^2/2)d\tau_2,$$

for some non-negative weights  $a$  and  $b$ . Unless otherwise specified, we assume  $b > a$  to avoid the excess shrinkage effect to zero. The other cases,  $b = a$  and  $b < a$ , are also discussed just for the completeness of theory.

The computation of normalizing function  $h$  is straightforward.

**Proposition 3.1** *The normalizing density  $h(x)$  is, if  $b > a$ ,*

$$h(x) = \frac{ab^2}{2(b^2 - a^2)}e^{-a|x|} \left\{ 1 - \left(\frac{a}{b}\right) e^{-(b-a)|x|} \right\} \quad (6)$$

and, if  $b = a$ ,

$$h(x) = \frac{a}{4}e^{-a|x|} \{1 + a|x|\}$$

The density of  $a < b$  is obtained by exchanging  $a$  and  $b$  in equation (6).

*Proof.* The following computation can be used for both  $b > a$  and  $b = a$ . In the mixture representation of the normalizing constant in equation (4), apply the change of variables as  $z = \tau_1 + \tau_2$  and  $w = \tau_1/(\tau_1 + \tau_2)$ . Integrate  $w$  out first, then  $z$ . The resulted function involves the Bessel function of the second kind with half-odd integers, which is simplified into the form above.  $\square$

Proposition 3.1 enables the evaluation of densities involving  $h(x)$ , such as the conditional density  $p(x|x')$  and the stationary density  $\pi(x)$ . In Figure 1, the conditional density  $p(x|x')$  with  $x' = 1$  and  $b = 1$  is plotted for the different choices of  $a$ . As weight  $a$  increases, the shrinkage effect to zero becomes visually clear. When  $a = b$ , the two shrinkage effects are completely balanced, which is expressed in the functional form of the density as the plateau between  $x'$  and zero. With this density as the prior, one does not discriminate any state between these two points a priori. In practice, however, we do not want the extreme amount of shrinkage to zero when transitioning the last state  $x'$  to the next  $x$  and, for this reason, we assume  $b > a$  in application. Figure 2 shows the marginal, stationary density  $\pi(x)$ . In general, the smaller  $a$  leads to the fatter tails, avoiding the shrinkage effect on the outliers. The spike around zero still exists even for the densities with small  $a$ , so the marginal shrinkage effect to zero is preserved. For large  $a$ , the density becomes more spiky, but it is clearly different from the double-exponential density. These characteristics of priors are revisited from the different viewpoints later in Section 3.2 for the better choice of hyperparameters.

In the expression of the second line of equation (6), note that  $(a/b)e^{-(b-a)|x|} < 1$  because  $b > a$  by assumption. It guarantees the absolute convergence of the series expression of the reciprocal normalizing function as

$$\frac{1}{h(x)} = \frac{2(b^2 - a^2)}{ab^2}e^{a|x|} \left\{ 1 - \left(\frac{a}{b}\right) e^{-(b-a)|x|} \right\}^{-1} = \frac{2(b^2 - a^2)}{ab^2}e^{a|x|} \sum_{n=0}^{\infty} \left(\frac{a}{b}\right)^n e^{-n(b-a)|x|}$$

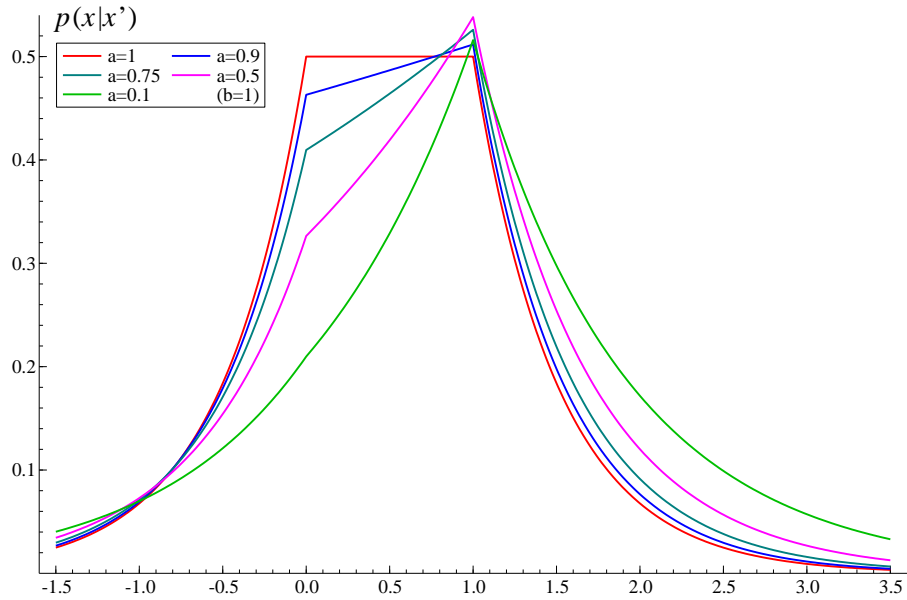


Figure 1: Conditional prior density of state  $p(x|x')$  for  $b = 1$ ,  $x' = 1$  and various  $a$ . If  $b = a$ , the plateau appears between two shrinkage points, which means that and the values between  $x'$  and zero are indifferent in the prior. As  $a$  becomes small, the shrinkage effect to  $x'$  dominates the functional form of the density, while some probability mass still remains around zero.

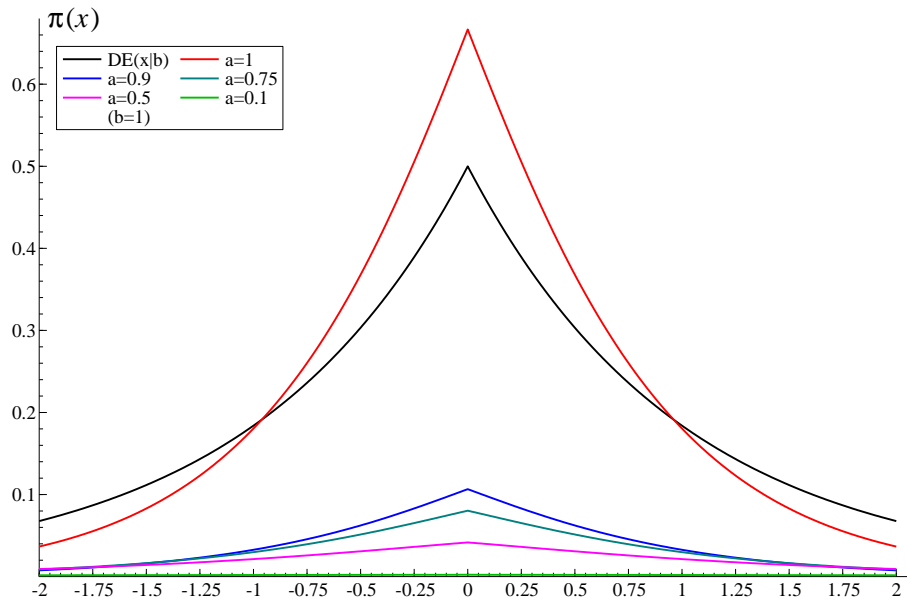


Figure 2: Marginal prior density of  $(w|x')$  for  $b = 10$  and various  $a$ . The smaller  $a$  is, the fatter tails the prior density becomes. The double-exponential prior density is also shown in the same figure. The density of the stationary distribution of the DFL process is clearly different from the double-exponential density for any  $a$ .

The reciprocal of the double exponential density with parameter  $a$  seen here will be canceled out with another  $f(x)$  function in the synthetic likelihood. The rest is the mixture of two components: (i) constant, for  $n = 0$ , which has no contribution to the posterior as the synthetic likelihood, and (ii) the discrete mixture of double exponential distributions with parameter  $n(b - a)$  for  $n > 0$ . In the second component, the mixture weight is proportional to the probability function of log-geometric distribution with parameter  $a/b$ , defined by the series representation of  $-\log(1 - a/b)$ . We summarize this observation as a proposition.

**Proposition 3.2** *If  $b > a$ , the reciprocal of normalizing function  $h$  is written as*

$$\frac{1}{h(x)} = \frac{2(a+b)(C_0 + C_+)}{b^2 DE(x|a)} q(x|a, b)$$

where  $q(x|a, b)$  is the mixture of a constant and the log-geometric mixture of double-exponential distributions,

$$q(x|a, b) = \frac{C_0}{C_0 + C_+} + \frac{C_+}{C_0 + C_+} \sum_{n=1}^{\infty} w_n DE(x|n(b-a)) \quad (7)$$

where  $C_0 = (b - a)/2$ ,  $C_+ = \log(b) - \log(b - a)$  and  $w_n = (a/b)^n / nC_+$ .

In the posterior computation, the component of the discrete mixture is interpreted as the double-exponential density with location  $x$  and parameter  $n(b - a)$ , or  $DE(z - x|n(b - a))$ , evaluated at  $z = 0$ . In other words, we separate this discrete mixture from the prior and interpret it as the part of the likelihood, or “synthetic” likelihood, where we generate  $n$  from the log-geometric distribution and, if  $n > 0$ , we pretend to observe  $z = 0$  with the double-exponential likelihood above. Note that the resulted posterior distribution is equivalent to the original prior. This transformation of the prior implies the CDLM representation, where we can benefit from the efficient computation by FFBS and the known conjugate modeling of other model parameters, such as stochastic volatility.

**Proposition 3.3** *If  $b > a$ , the joint distribution of the DFL prior can be computed as the posterior of the following conditional dynamic linear model; the state evolution and the process of the associated latent parameter are*

$$\begin{aligned} x_t | x_{t-1}, \lambda_{b,t} &= x_{t-1} + N(0, \lambda_{b,t}) \\ \lambda_{b,t} &\sim Ga(1, b^2/2) \end{aligned} \quad (8)$$

with the initial distribution at  $t = 1$ ,

$$\begin{aligned} x_1 | \lambda_{a,1} &\sim N(0, \lambda_{a,1}) \\ \lambda_{a,1} &\sim Ga(1, a^2/2) \end{aligned}$$

The synthetic observation is defined as, at  $t = T$ ,

$$\begin{aligned} z_T | \lambda_{a,T} &\sim N(x_T, \lambda_{a,T}), \quad z_T = 0 \\ \lambda_{a,T} &\sim Ga(1, a^2/2) \end{aligned}$$

For  $t \in 2:(T - 1)$ , the latent count  $n_t$  follows the discrete distribution

$$n_t \sim \frac{C_0}{C_0 + C_+} 1[n_t = 0] + \frac{C_+}{C_0 + C_+} \text{log-Geo}(a/b), \quad (9)$$



where  $1[n_t = 0]$  here is the point mass on  $n_t = 0$  and  $\text{log-Geo}(a/b)$  is the discrete distribution on positive integers  $\{1, 2, \dots\}$  whose probability function is  $\text{Pr}[n_t = n] = w_n$ . The quantities such as  $w_n$ ,  $C_0$  and  $C_+$  are defined in Proposition 3.2. Conditional on  $n_t > 0$ , we additionally have observational equation defined by,

$$\begin{aligned} z_t | x_t, \lambda_{n,t} &\sim N(x_t, \lambda_{n,t}), & z_t &= 0 \\ \lambda_{n,t} | n_t &\sim \text{Ga}(1, n_t^2(b-a)^2/2) \end{aligned} \quad (10)$$

For  $n_t = 0$ , we have no additional observation equation of  $z_t$ , and  $\lambda_{n,t}$  can follow any prior distribution.

In this augmented joint distribution of state variables, the shrinkage effects of the new Markov process gains new interpretation. If  $n_t = 0$  is sampled at time  $t$ , then the model has no synthetic observation at  $t$ , or  $z_t$  is “missing.” If  $n_t > 0$  is sampled, then  $z_t = 0$  is observed and the state variable is affected by this additional information that encourages the shrinkage to zero at time  $t$ . This is exactly the “local/vertical” shrinkage effect, that is different from the global/horizontal shrinkage that is uniformly applied to the state variables at all the time points, as pointed out by Uribe and Lopes (2017). The amount of this shrinkage is indirectly controlled by weights  $a$  and  $b$ ; the larger  $b$  is, the more likely it is that  $n_t = 0$ , having less shrinkage effect to zero, which is consistent with the interpretation of weights in the loss function.

*Proof.* Propositions 3.1 and 3.2 prove the geometric series representation of the transition density as

$$p(x_t | x_{t-1}) = \frac{f(x_t)g(x_t, x_{t-1})}{f(x_{t-1})} \frac{2(C_0 + C_+)(a+b)}{b^2} q(x_{t-1} | a, b)$$

where  $q(x_{t-1} | a, b)$  is the discrete mixture given in equation (7). With the latent variable  $n_{t-1}$  in the mixture representation, the transition density is understood as the marginal of  $(x_t, n_{t-1})$ . Marginally,  $n_{t-1} = 0$  with probability  $C_0/(C_0 + C_+)$ , and  $n_{t-1} > 0$  with probability  $C_+/(C_0 + C_+)$ . Jointly, for  $n_t = 0$ ,

$$p(x_t, n_{t-1} = 0 | x_{t-1}) = \frac{f(x_t)g(x_t, x_{t-1})}{f(x_{t-1})} \frac{b^2 - a^2}{b^2}$$

and, for  $n_t > 0$ ,

$$p(x_t, n_{t-1} | x_{t-1}) = \frac{f(x_t)g(x_t, x_{t-1})}{f(x_{t-1})} \frac{2(a+b)}{b^2} \frac{1}{n_{t-1}} \left(\frac{a}{b}\right)^{n_{t-1}} DE(x_{t-1} | n_{t-1}(b-a))$$

For notational convenience, we define  $w(n)$  by

$$w(n) = \frac{2(a+b)}{b^2} \left\{ \frac{b-a}{2} 1[n=0] + \frac{1}{n} \left(\frac{a}{b}\right)^n 1[n>0] \right\}$$

In the joint density of state  $x_{1:T}$  and auxiliary variable  $n_{2:(T-1)}$ , observe that  $f(x_t)$  appears both in the numerator and denominator for  $t = 2, \dots, T-1$  and cancels out one another as

$$\begin{aligned} p(x_{1:T}, n_{2:(T-1)}) &= \pi(x_1) p(x_2 | x_1) \prod_{t=3}^T p(x_t | x_{t-1}) \\ &= \pi(x_1) \frac{f(x_2)g(x_2, x_1)}{h(x_1)} \prod_{t=3}^T \frac{f(x_t)g(x_t, x_{t-1})}{f(x_{t-1})} w(n_{t-1}) \prod_{\substack{t=3:T \\ n_{t-1}>0}} DE(x_{t-1} | n_{t-1}(b-a)) \quad (11) \\ &= f(x_1) f(x_T) \prod_{t=2}^T g(x_t, x_{t-1}) \prod_{t=2}^{T-1} w(n_t) \prod_{t:n_t>0} DE(x_t | n_t(b-a)), \end{aligned}$$

where  $\{t : n_t > 0\}$  means that the product is taken only for  $t \in 2 : (T - 1)$  that satisfies  $n_t > 0$ . Using the scale mixture representation of double exponential distributions, we can read off in equation (11) the conditional distribution,

$$p(x_{1:T}|n_{2:(T-1)}, \Lambda_T) = \left\{ N(0|x_T, \lambda_{a,T}) \prod_{t:n_t>0} N(0|x_t, \lambda_{n,t}) \right\} \left\{ N(x_1|0, \lambda_{a,1}) \prod_{t=2}^T N(x_t|x_{t-1}, \lambda_{b,t}) \right\}$$

where  $\Lambda_T$  is the set of all the latent variables up to time  $T$ , i.e.,  $\Lambda_T = \{\lambda_{a,1}, \lambda_{a,T}, \lambda_{b,2:T}, \lambda_{n,2:(T-1)}\}$ . The densities in the first parenthesis imply the linear and Gaussian likelihood, and those in the second parenthesis are the Gaussian AR(1) prior. This is exactly a dynamic linear model conditional on all the latent variables, the joint density of which is given by

$$p(n_{2:(T-1)}, \Lambda_T) = \prod_{t=1, T} G a(\lambda_{a,t}|1, a^2/2) \prod_{t=2}^T G a(\lambda_{b,t}|1, b^2/2) \prod_{t=2}^{T-1} w(n_t) \prod_{t:n_t>0} G a(\lambda_{2t}|n_t^2(a-b)^2/2)$$

As a whole, this is exactly the CDLM of the proposition.  $\square$

In section 4.2, weight parameters  $(a, b)$  are also estimated. For the computation of the conditional posterior of weights, the state density in equation (11) is simplified as follows.

**Proposition 3.4** *As the function of  $(a, b)$ , the joint density of states and latent counts is written as*

$$p(x_{1:T}, n_{2:(T-1)}) \propto f(x_1)f(x_T) \left(\frac{b^2 - a^2}{b^2}\right)^{T-2} \prod_{t=2}^T g(x_t, x_{t-1}) \prod_{t:n_t>0} \left(\frac{a}{b}\right)^{n_t} e^{-n_t(b-a)|x_t|}$$

**Remark 3.1** If  $a = b$ , the reciprocal of the normalizing function has the integral representation,

$$\frac{1}{h(x)} = \frac{4}{a} e^{a|x|} \{1 + a|x|\}^{-1} = \frac{2}{DE(x|a)} \int_0^\infty e^{-(1+a|x|)\phi} d\phi$$

and is understood as the mixture of double-exponential distribution with the latent parameter  $\phi$ . Although not discussed further in this paper, the corresponding synthetic model can be found even in this case and utilized for the posterior computation.

### 3.2 Subjective elicitation of weight parameters

The weights  $a$  and  $b$  determine the structure of sparsity in the model. As the hyperparameters, these weights must be carefully chosen so that the prior appropriately reflects one's belief on the dynamics and sparsity of the state variables. One approach to the choice of hyperparameters is to specify the conditional mean of the state transition in equation (5). This density is the location-scale mixture of the Gaussian AR(1) process,

$$p(x|x') = \int_0^\infty \int_0^1 N(x|wx', w(1-w)z) q(\tau, w) dz dw, \quad (12)$$

where the mixing distribution is

$$q(z, w) = \frac{N(x'|0, z) a^2 b^2}{h(x')} \frac{1}{4} z e^{-\frac{b^2}{2}z} e^{-\frac{(b^2-a^2)}{2}wz}, \quad (13)$$

which is obtained by change of variables with  $z = \tau_1 + \tau_2$  and  $w = \tau_1/(\tau_1 + \tau_2)$ . The conditional expectation  $E[x|x'] = E[w|x']x'$  is one of the useful information that statisticians can interpret as ‘‘conditional shrinkage effect’’ and elicit their prior belief based on this quantity. The distribution  $q(z, w)$  itself is analytically available as well and provides further information on one's prior belief.

**Proposition 3.5** For DFL prior with  $b > a$ , the conditional transition density in equation (12) has the mean  $E[w|x']x'$ , where

$$E[w|x'] = \frac{1 - \frac{2a}{(b^2 - a^2)|x'|} (1 - e^{-(b-a)|x'|})}{1 - \frac{a}{b} e^{-(b-a)|x'|}} \quad (14)$$

The joint distribution in equation (13) is decomposed into the compositional form. The conditional distribution of  $(z|w)$  is  $GIG(3/2, wa^2 + (1-w)b^2, (x')^2)$  and the marginal density of  $w$  is

$$q(w) = \frac{a^2 b^2}{4h(x')} e^{-|x'| \sqrt{wa^2 + (1-w)b^2}} \left\{ \frac{|x'|}{wa^2 + (1-w)b^2} + \frac{1}{(wa^2 + (1-w)b^2)^{3/2}} \right\} \quad (15)$$

See the appendix for the computation to prove these results.

The conditional mean  $E[x|x']$  in equation (12) is plotted against  $x'$  in Figure 3a. When  $a$  is small, the conditional means are almost on the diagonal line, showing more shrinkage effect to  $x'$  as in the random walk models. In contrast, for large  $a$ , the shrinkage effect to zero becomes strong, making the conditional means off the diagonal line in the figure. The conditional mean is the non-linear function of  $x'$  as shown in equation (14), and this non-linearity is also visually confirmed in the figure. Figure 3b depicts the density of shrinkage effect  $q(w)$  in equation (15), conditional on  $x' = 1$ , with  $z$  marginalized out. For all the values of  $a$  examined here, the prior mass concentrates around  $w \approx 1$ , implying the dominating conditional shrinkage effect is directed to  $x'$ , not to zero. For smaller  $a$ , however, the more probability mass is placed on the smaller values of  $w$  as well.

These two figures are just one aspect of the prior structure; for different choices of  $(a, b, x')$ , the conditional prior mean and density look completely different, and it is difficult to summarize those differences in a simple manner. This might be the potential difficulty in subjectively specifying the prior, which motivates the estimation of hyperparameters. The automatic adjustment of hyperparameters via posterior analysis is discussed later in Section 4.2, but the choice of hyperparameters based on the discussion here still remains important.

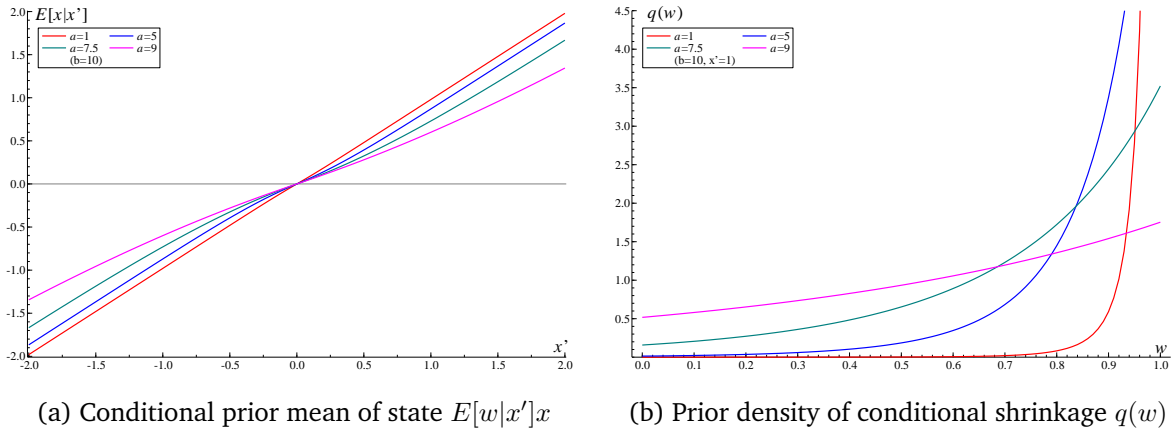


Figure 3: Left: Conditional prior mean  $E[x|x'] = E[w|x']x'$  for  $b = 10$  and various  $a$  as the function of  $x'$ . The larger  $a$  is, the more shrinkage to zero is observed. Conversely, if  $a$  is small enough, then  $E[x|x'] \approx x'$ . The shrinkage effect is also dependent on  $x'$  in non-linear way. Right: Prior density of  $(w|x')$  for  $b = 10$  and various  $a$  with  $z$  marginalized out. Small  $a$  implies  $w \approx 1$  with high probability, having little shrinkage to zero. For large  $a$ , it is still likely that  $w$  is close to unity, but more probability mass is on smaller values of  $w$ , resulting in the additional shrinkage to zero.

### 3.3 Simulation from the prior

Simulating the random variable  $x$  from the conditional distribution  $p(x|x')$  is an important step at the one-step and multi-step ahead predictions. The location-scale mixture representation in equation (12) enables the simulation from the normal distribution  $N(wx', w(1-w)z)$ , given that  $(z, w)$  is sampled from  $q(z, w)$ . Proposition 3.5 provides the compositional form of this joint density, in which  $q(z|w)$  is the generalized inverse Gaussian distribution and relatively easy to sample from (e.g., Devroye 2014).

The problem remains in the sampling of  $w$  from marginal  $q(w)$  in equation (15). The density of  $w$  is transformed into the relatively simple form by taking another scale.

**Proposition 3.6** *The marginal density of  $q(w)$  is expressed in the scale of  $y = |x'|\sqrt{wa^2 + (1-w)b^2}$  as*

$$q(y) = \frac{ab|x'|}{be^{-a|x'|} - ae^{-b|x'|}} \{y^{-1}e^{-y} + y^{-2}e^{-y}\}, \quad (16)$$

where  $y \in (a|x'|, b|x'|)$ . The distribution function is

$$Q(y) = \int_{a|x'|}^y q(t)dt = \frac{be^{-a|x'|} - (ab|x'|)y^{-1}e^{-y}}{be^{-a|x'|} - ae^{-b|x'|}} \quad (17)$$

The explicit formula of distribution function helps computing the inverse distribution function numerically, thus allows the inverse sampling. See more details in the appendix.

### 3.4 Interpretation of shrinkage effects

The DFL prior is characterized by the two conflicting shrinkage effects to the previous state and zero that are not seen in the other shrinkage priors used in the time series analysis. Proposition 3.3 gives these shrinkage effects the new interpretation; the shrinkage to  $x_{t-1}$  is based on the state equation (8), while the shrinkage to zero is achieved by the synthetic observations in (10). The former has been seen in the literature of DLMS with shrinkage priors, where the state transition is defined by

$$p(x_t|x_{t-1}, \tau_{2t}, b) = N(x_t|x_{t-1}, \tau_{2t})$$

If  $\tau_{2t}$  follows the gamma distribution with shape 1, then this is the special case of DFL prior with  $a = 0$ . Another example is the case where  $\tau_{2t} = \tau_2$  and follows the half-Cauchy prior or its mixture (Frühwirth-Schnatter and Wagner 2010, Belmonte et al. 2014 and Bitto and Frühwirth-Schnatter 2019). As discussed already, the shrinkage effect of this prior is limited for its constant scale  $\tau_2$ ; it has been improved by Kalli and Griffin (2014), Uribe and Lopes (2017) and Kowal et al. (2019). In all the examples here, the prior consists of a single shrinkage effect to the previous state. The DFL prior is clearly different from those in adding the new shrinkage effect to zero.

Another shrinkage model that should be considered for the comparison with the DFL prior, is the existing fused LASSO prior in Kyung et al. (2010) applied to the joint distribution of state variables (the joint fused LASSO prior, or JFL). The joint distribution of  $T$  states variables is modeled as

$$p(x_{1:T}|a, b) \propto \exp \left\{ -a \sum_{t=1}^T |x_t| - b \sum_{t=1}^T |x_t - x_{t-1}| \right\} \quad (18)$$

This density has the similar, but simpler, synthetic model representation as

$$p(x_{1:T}|a, b) \propto \underbrace{\left\{ \prod_{t=1}^T DE(z_t - x_t|a) \right\}}_{\text{“likelihood”}} \underbrace{\left\{ \prod_{t=1}^T DE(x_t - x_{t-1}|b) \right\}}_{\text{“prior”}},$$

where  $z_t = 0$  for all  $t$ . The model becomes a CDLM with the scale mixture augmentation of the double-exponential distributions. However, the JFL model lacks several desired properties that the proposed DFL possesses. First, the flexibility of the JFL prior in shrinkage effect is limited. This is indicated in the difference of the DFL/JFL priors in the synthetic likelihood; while the DFL prior allows for the possibility of missing the synthetic observation and the shrinkage effect to zero can vary across time based on the value of  $n_t$ , the latent  $z_t$  in the JFL model is always observed, and its shrinkage effects are equally controlled by parameter  $a$  at any time point. In this sense, the flexibility of the JFL model in local shrinkage is limited. Second, the normalizing constant of the JFL prior in (18) is unknown. This does not involve the state variables, but weight parameters  $(a, b)$ , so the the posterior analysis on weights is infeasible at this point, unlike the model with the DFL prior. At last, but most importantly, predictive analysis is not available with the JFL prior. The joint density of the JFL prior does not specify the evolution of state variables and the existence of state variables after  $T$  in the model is not assumed. If one defines the joint distributions of  $x_{1:T}$  and  $x_{1:T+1}$  by (18) individually, then

$$\int p(x_{1:(T+1)}|a, b)dx_{T+1} \neq p(x_{1:T}|a, b),$$

and the conditional density is not coherently defined after  $T$ . This concludes that the JFL prior is not suitable for the formal sequential and predictive analysis.

### 3.5 Baseline of prior process

The marginal prior mean of states is set to be zero in order that the additional shrinkage is directed to zero. The point of shrinkage can be changed from zero to any value (or baseline) and, in fact, estimated with some prior. Denote this baseline by  $\mu$ , and modify the transition density of the DFL process as

$$p(x_t|x_{t-1}, \mu) = \frac{f(x_t - \mu)g(x_t, x_{t-1})}{h(x_{t-1} - \mu)}$$

The same augmentation of the model can be applied to this case. The only difference is that the value of the synthetic observation is now the baseline, i.e.,  $z_t = \mu$ . The baseline is the location parameter in the synthetic likelihoods,  $z_t \sim N(x_t, \lambda_{n,t})$  with  $z_t = \mu$ , and the prior at  $t = 1$ ,  $x_1 \sim N(\mu, \lambda_{a,1})$ . We use the normal prior for the baseline, that is conditionally conjugate in the synthetic model. Alternatively, one can choose the double-exponential/horseshoe prior to introduce the shrinkage effect on the baseline.

## 4 Application to state-space modeling

### 4.1 Estimation by Markov chain Monte Carlo

Consider the Gaussian and linear likelihood of the state space model given by

$$p(y_t|\theta_t) = N(y_t|F_t'\theta_t, V_t), \tag{19}$$

where  $F_t$  is  $p \times 1$  vector of predictors known at time  $t$ ,  $\theta_t = (\theta_{1t}, \dots, \theta_{pt})'$  is the vector of state variables and  $V_t$  is the observational variance parameter modeled later in Section 4.3. Each state variable independently follows the DFL process,

$$p(\theta_{it}|\theta_{i,t-1}) \propto \exp\{-a_i|\theta_{it} - \mu_i| - b_i|\theta_{it} - \theta_{i,t-1}|\} \tag{20}$$

where the baseline and weights are customized for each predictor  $i$  and denoted by  $\mu_i$  and  $(a_i, b_i)$ . The CDLM representation of the prior given in Proposition 3.3 is now combined with the ‘‘real’’ likelihood in

(19). Following the notation in Proposition 3.3, the set of all the latent variables introduced for this state variable for the  $i$ -th state  $\{\theta_{it}\}$  is denoted by  $\{\Lambda_{i,T}, n_{i,2:(T-1)}\}$ . The algorithm of Gibbs sampler for the posterior inference can be derived easily from the CDLM representation.

---

### Gibbs sampler for the Bayesian dynamic fused LASSO models

1. Sampling  $\theta_{1:T}$  by forward filtering and backward sampling (FFBS).

The conditional posterior of  $\theta_{1:T}$  is equivalent to the posterior of the conditionally dynamic linear model with “real” likelihood in (19) and the following “synthetic” likelihoods and prior. For each  $t \in 2 : (T - 1)$ , if  $n_{it} > 0$ , then the model has the synthetic likelihood,

$$z_{it}|\theta_{it} \sim N(\theta_{it}, \lambda_{n,it}), \quad z_{it} = \mu_i$$

At  $t = T$ , the model always has the synthetic likelihood,

$$z_{iT}|\theta_{iT} \sim N(\theta_{iT}, \lambda_{a,iT}), \quad z_{iT} = \mu_i$$

The state evolution of the CDLM is defined by the synthetic prior; for  $t > 1$ ,

$$\theta_{it}|\theta_{i,t-1} \sim N(\theta_{i,t-1}, \lambda_{b,it}),$$

and, for  $t = 1$ ,

$$\theta_{i1} \sim N(\mu_i, \lambda_{a,i1}),$$

By FFBS, one can sample from the full posterior of  $\theta_{1:T}$  of this CDLM (e.g., West 1984, Chap. 4.8).

2. Sampling  $\Lambda_{1:p,T}$ .

They are independently sampled from

$$\begin{aligned} \lambda_{a,it} &\sim GIG(1/2, a_i^2, (\theta_{it} - \mu_i)^2), \quad \text{for } t = 1, T \\ \lambda_{n,it} &\sim GIG(1/2, \{n_{it}(b_i - a_i)\}^2, (\theta_{it} - \mu_i)^2), \quad \text{for } t \in \{2, \dots, T - 1\} \text{ and } n_{it} > 0 \\ \lambda_{b,it} &\sim GIG(1/2, b_{it}^2, (\theta_{it} - \theta_{i,t-1})^2), \quad \text{for } t = 2, \dots, T \end{aligned}$$

If  $n_{it} = 0$ , then  $\lambda_{n,it}$  is missing and not sampled at this iteration. See the following Remark 4.1.

3. Sampling  $n_{1:p,2:(T-1)}$ .

The sampling of  $n_{it}$  is based on the conditional posterior with  $\lambda_{n,it}$  marginalized out. For  $i \in 1 : p$  and  $t \in 2 : (T - 1)$ , the latent counts,  $n_{it}$ 's, are independently sampled from

$$n_{it} \sim Geo\left(\frac{a_i}{b_i} e^{-(b_i - a_i)|\theta_{it} - \mu_i|}\right),$$

where  $Geo(q)$  means the geometric distribution; for  $N \sim Geo(q)$ , for  $Pr[N = n] = (1 - q)q^n$  and  $n \in \{0, 1, 2, \dots\}$ . This marginalization not only simplifies the sampling procedure but also facilitates the mixing of Markov chain (partially collapsed Gibbs sampler, Van Dyk and Park 2008).

---

**Remark 4.1** If  $n_{it} = 0$  is sampled for some  $i$  and  $t$ , then the synthetic likelihood of  $\lambda_{n,it}$  is missing, and  $\lambda_{n,it}$  must be sampled from its prior. As noted in Proposition 3.3, one can use any prior distribution for  $(\lambda_{n,it}|n_{it} = 0)$ , yet the mixture representation is still valid. In fact, the value of  $\lambda_{n,it}$  does not affect any of the other sampling steps if  $n_{it} = 0$ . For this reason, whenever  $n_{it} = 0$  is sampled, one does not have to generate  $\lambda_{n,it}$  and leave it to the missing state.

## 4.2 Estimation of hyperparameters

In practice, tuning all the weight parameters  $\{a_i, b_i\}_{i=1:p}$  is not realistic. It is desirable if the automated adjustment of those hyperparameters is fully or partially available. The formal approach to this goal is the Bayesian posterior analysis by placing the prior distribution on the hyperparameters. To emphasize that those hyperparameters are now to be estimated, replace the constant weights  $(a_t, b_i)$  by random variables  $(\alpha_i, \beta_i)$  for  $i = 1 : p$ .

To consider this problem, denote one of the state variables by  $x_t$  again for the notational simplicity. It follows the DFL process with weights  $\alpha$  and  $\beta$ , where  $0 < \alpha < \beta$ . Also, for the convenience of estimation and interpretation, we re-parametrize the weights by  $\alpha = \rho\beta$  with  $\rho \in (0, 1)$ , so that the assumed inequality always holds. The joint density of state variables in Proposition 3.4 as the function of  $(\alpha, \beta)$  is

$$\begin{aligned} p(x_{1:T}|n_{2:(T-1)}, \alpha, \beta) &\propto f(x_1)f(x_T) \prod_{t=2}^T g(x_t, x_{t-1}) \left(\frac{\beta^2 - \alpha^2}{\beta^2}\right)^{T-2} \prod_{t:n_t>0} \left(\frac{\alpha}{\beta}\right)^{n_t} e^{-n_t(\beta-\alpha)|x_t|} \\ &\propto \rho^{2+\sum n_t} (1-\rho^2)^{T-2} \beta^{T+1} \exp \left\{ -\rho\beta(|x_1| + |x_T|) - \beta \sum_{t=2}^T |x_t - x_{t-1}| - (1-\rho)\beta \sum_{t:n_t>0} n_t|x_t| \right\}, \end{aligned}$$

where the product and summation of  $n_t$  are applied to  $t \in 2 : (T-2)$  that satisfies  $n_t > 0$ . For this likelihood, the conditionally conjugate prior for  $\beta$  is the gamma distribution. If  $\beta \sim Ga(r_0^b, c_0^b)$ , then the conditional posterior of  $\beta$  is  $Ga(r^b, c^b)$ , where

$$r^b = r_0^b + T + 2 \quad \text{and} \quad c^b = c_0^b + \rho(|x_1| + |x_T|) + \sum_{t=2}^T |x_t - x_{t-1}| + (1-\rho) \sum_{t:n_t>0} n_t|x_t|$$

The full conditional posterior density of  $\rho$  is given by, with the prior density  $\pi(\rho)$ ,

$$p(\rho|-) \propto \pi(\rho) \rho^{2+\sum n_t} (1-\rho^2)^{T-2} \exp \left\{ -\rho \left( \beta(|x_1| + |x_T|) - \beta \sum_{t:n_t>0} n_t|x_t| \right) \right\}$$

In this research, we pursue the simplicity of computation by using the discrete prior on the interval  $(0, 1)$ . For some positive integer  $N$  and  $M$  ( $M < N$ ), the grid is defined by  $d = 1/N$  and the prior support of  $\rho$  is  $\{d, 2d, \dots, Md\}$ . In practice, it is advised to avoid the value  $Md$  not too close to 1, e.g.,  $Md = 0.9$ , for the numerical issue. To consider the possibility of  $\rho$  close to unity more rigorously, it is necessary to include the case  $a = b$  explicitly in the set of models; see Remark 3.1. In our analysis,  $d = 0.001$  ( $N = 1000$ ),  $M = 900$  and  $\rho$  follows the discrete uniform distribution on  $\{d, 2d, \dots, Md\}$ . The prior probabilities on those points are proportional to the beta density  $Be(a_0^r, b_0^r)$  evaluated on the grids.

The careful, subjective choice of hyperparameters in the prior of  $(\beta, \rho)$  is still unavoidable for the appropriate representation of one's prior belief. To see this point, the marginal prior densities of  $\alpha$  and  $w$  are drawn in Figure 4a and 4b, respectively, for different choices of hyperparameters  $b_0^r = 1, 2, 5, 10$ , while the other parameters are fixed as  $a_0^r = 1$ ,  $(r_0^b, c_0^b) = (1, 0.1)$  and  $x_{t-1} = 1$ . As clearly seen in the prior of  $\alpha$  in Figure 4a, the larger  $b_r$  is, the less weight is placed on the shrinkage effect toward zero. The difference of those hyperparameters is emphasized in the density of  $w$ —the conditional shrinkage effect to  $x_{t-1}$  defined in the location-scale mixture representation in (12). In Figure 4b, the density with  $b_r = 1$  shows the fatter tail in smaller values of  $w$ , implying the excess shrinkage effect to zero, even though the strong signal is assumed by  $x_{t-1} = 1$ . From this viewpoint, although this choice means  $\rho$  follows the uniform distribution and is seemingly “less informative” prior, it is in fact regarded an extreme choice for its strong shrinkage effect applied to even large value of  $x_{t-1}$ .

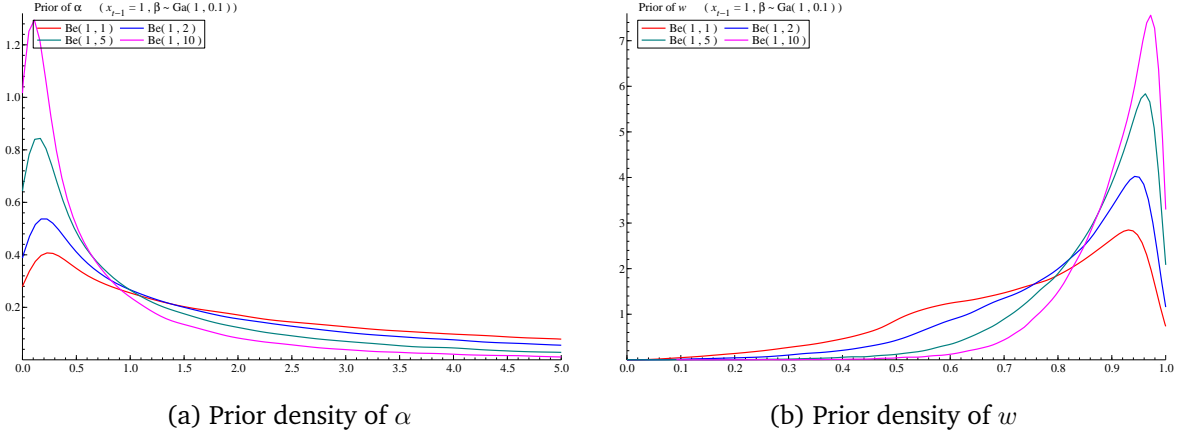


Figure 4: Left: the density of  $\alpha = \rho\beta$  when  $\rho \sim Be(1, b_0^r)$  and  $\beta \sim Ga(1, 0.1)$ , Right: the density of  $w = \tau_1/(\tau_1 + \tau_2)$  conditional on  $x_{t-1} = 1$ . The larger  $b_0^r$  is, the more prior mass concentrates around smaller  $\rho$  (and  $\alpha$ ) as seen in the left figure. This property is inherited to the densities of  $w$  in the right figure; the large  $b_0^r$  (i.e., small  $\rho$  and  $\alpha$ ) makes the density of  $w$  skewed toward unity, implying the stronger shrinkage of  $x_t$  to  $x_{t-1}$ , not to zero. Note that  $x_{t-1} = 1$  in these figures; if this value of the state variable is regarded an significant signal, then choosing small  $b_0^r$  (e.g.,  $b_0^r = 1$ ) and shrinking the next state  $x_t$  to zero are not appropriate. The densities are computed by simulation based on 10,000 samples of  $(\rho, \beta)$  in both figures.

The baseline is the location parameter of the synthetic likelihoods and the prior of initial state  $x_1$ . The normal prior for  $\mu$  is conditionally conjugate; for  $\mu \sim N(m_0, \sigma_0^2)$ , the conditional posterior of  $\mu$  is  $N(m_1, \sigma_1^2)$ , where

$$\sigma_1^{-2} = \frac{1}{\sigma_0^2} + \frac{1}{\lambda_{a,1}} + \frac{1}{\lambda_{a,T}} + \sum_{t:n_t>0} \frac{1}{\lambda_{n,t}} \quad \text{and} \quad \frac{\mu_1}{\sigma_1^2} = \frac{m_0}{\sigma_0^2} + \frac{x_1}{\lambda_{a,1}} + \frac{x_T}{\lambda_{a,T}} + \sum_{t:n_t>0} \frac{x_t}{\lambda_{n,t}}$$

Shrinkage on this baseline can be introduced by another hierarchical prior on  $\sigma^2$ .

### 4.3 Modeling of stochastic volatility

The observational variance  $V_t$ , or stochastic volatility, can also be modeled and estimated. If the stochastic volatility appears only in observational equation (19), the MCMC algorithm in Section 4.1 is easily extended by incorporating the sampling of this parameter. For the Gaussian likelihood in equation (19), the inverse-gamma type prior is useful for its conditional conjugacy. The examples include the constant variance  $V_t = V$  for all  $t$  with the conjugate inverse-gamma prior. Another model is the log-Gaussian models where  $\log(V_t)$  follows the Gaussian AR(1) process. Although the conditional posterior is not any well-known distribution, many computational methods are available for this model, e.g., mixture sampler (Kim et al. 1998 and Omori et al. 2007).

In contrast, the “scale-free” dynamic linear models include  $V_t$  in the state equation to scale the observational and state variances simultaneously. The conjugate prior on  $V_t$  in the DLMS of this type is the inverse gamma-scaled beta process; if  $V_t = V$  for all  $t$ , it reduces to the inverse gamma prior (West and Harrison 1997, Chap. 4.5 and 10.8). The DFL process in equation (1) is applied to the scaled state variable  $x_t/\sqrt{V}$ ; this affects the variance of the synthetic likelihood and prior but not the other parts of the model. Consequently, variance parameter  $V$  appears in the synthetic likelihoods and prior of the CDLM representation in Section 4.1 as their scales, for which the FFBS is available to sample from



the conditional joint posterior of states and observational variance. We assume the case of constant variance,  $V_t = V$  for all  $t$ , and use the conjugate inverse gamma prior,  $V^{-1} \sim Ga(n_0/2, n_0 S_0/2)$ . For the computational details, see the appendix.

## 5 Illustration via data analysis

The posterior analysis by the DLM with the DFL prior is conducted for the simulated and real datasets. In the simulation study, the proposed model is compared with the standard dynamic models with double-exponential priors to clarify the difference in their shrinkage effects. In the analysis of real macroeconomic data, the shrinkage by the DFL priors shows the similarity to the dynamic variable selection by the latent threshold models.

All computations are implemented by Ox (Doornik, 2007).

### 5.1 Simulated dataset

The purpose of the study in this subsection is the illustration and comparative analysis of the proposed and existing models. The univariate time series  $\{y_t\}$  is generated from (19), based on the following predictors and the true values of the parameters. Twelve predictors are generated from the uniform distribution on  $(0, 2)$ , except for the first predictor as the intercept. The first four predictors are “active” and the others are “inactive”, in the sense that the coefficients of the former are non-zeros for all/some  $t$  and the others are always zero, creating the over-parametrized but sparse linear model as the data generating process. The data process  $\{y_t\}$  is plotted in Figure 5a, with the coefficients of the four active predictors  $\{\theta_{1:4,t}\}$  in 5b. The true value of the observational variance is  $V_t = V = 1.5$ .

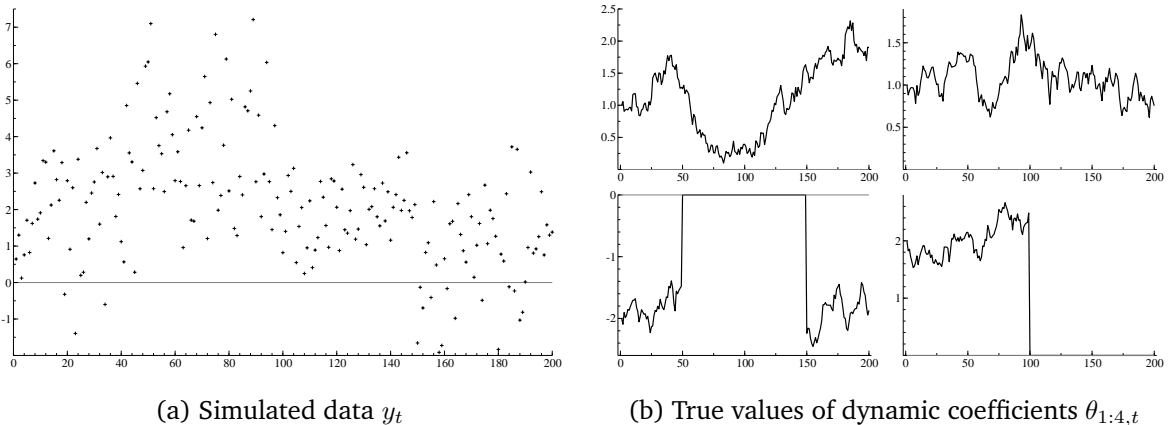


Figure 5: Left: the simulated time series  $\{y_t\}_{t=1:T}$  with  $T = 200$ . Right: the true values of dynamic coefficients  $\theta_{1:4,t}$ . The first predictor is constant and unity (intercept). The third and fourth predictors are temporarily inactive, i.e., the coefficients become exact zero in certain periods;  $\theta_{3t} = 0$  for  $50 \leq t < 150$  and  $\theta_{4t} = 0$  for  $t > 100$ . The other predictors do not contribute to the prediction of  $y_t$  at all, i.e.,  $\theta_{it} = 0$  for all  $t$  and  $i \in \{5, 6, \dots, 12\}$ .

For the analysis of this dataset, in addition to the DFL prior, we also consider the double-exponential (DE) prior, i.e., the DFL with  $a = 0$ . The DLMs with those priors are named as DFL-DLMs and DE-DLMs. These dynamic models share the same likelihood in (19) and differ in the modeling of state evolution. The observational variance is assumed to be constant over time,  $V_t = V$  for all  $t$ , and to follow inverse

gamma prior  $V^{-1} \sim Ga(n_0/2, n_0 S_0/2)$ . We set  $n_0 = 1$  and  $S_0 = 1$  in all the models. For baseline  $\mu_i$ , we set  $\mu_i = 0$  or  $\mu_i : iid \sim N(0, 10^2)$ . The weight parameters  $\beta_i$ 's follow the independent gamma priors as  $\beta_i : iid \sim Ga(1, 0.1)$  in both models. In the DFL-DLMs, the other weight parameter follows (i)  $\rho_i : iid \sim Be(1, 2)$ , (ii)  $Be(1, 5)$  or (iii)  $Be(1, 10)$ . In the DE-DLMs, the initial state at  $t = 1$  is modeled as  $\theta_{i1} \sim DE(\mu_i | \alpha_i)$  for the fair comparison with the DLF-DLMs. The three sets of hyperparameters are used: (i)  $\alpha_i \sim Ga(1, 0.1)$ , (ii)  $Ga(0.5, 0.5)$  and (iii)  $Ga(1, 10)$ . The posteriors are computed based on 5,000 iterations after 500 burn-in period. In predictive analysis, the posterior computation by the MCMC method is repeated for different set of data  $y_{1:s}$  for each  $s$ , including the estimation of the model parameters  $(\beta_i, \rho_i)$ , to generate  $y_{s+1}$  from the one-step ahead predictive distribution during the iterations of MCMC and compute the point forecast  $E[y_{s+1} | y_{1:s}]$ . In each analysis, the number of iterations in MCMC is 2,000 with 200 burn-in.

## Posterior and predictive results

The posterior analyses of all the twelve models with various DFL/DE priors are summarized by the mean squared errors (MSEs) of dynamic coefficients and one-step ahead predictions in Table 1. The computation of MSEs starts at  $t = 25$ , because the posteriors of DE-DLM with baseline zero are strongly biased to zero before this point, as seen later in Figure 8a. Among the models listed in the table, the DFL-DLMs with baseline zero perform best in almost all of those measures. Even though the baseline is fixed to zero, the posterior trajectories of active state variables can track the trends of the true coefficients correctly, partly for the adaptive weight parameters  $\alpha_i$ . For this reason, the baselines are nuisance parameters for DFL-DLMs in this example. In contrast, the MSEs of the active state variables for DE-DLMs are large due to the strong penalty on the dynamics assumed in the prior. The fitting of DE-DLMs to data is improved by the introduction of baseline parameters, which instead increases the uncertainty in estimation and prediction. The notable difference between DFL-/DE-DLMs is seen in the MSE of the inactive state variables, where the MSEs of DFL-DLMs with no baseline parameters are extremely small for the additional shrinkage effect to zero. This property is visually confirmed later in Figure 8b. In the following, we focus on  $\mathcal{M}_3$  and  $\mathcal{M}_9$ , the best DFL-/DE-DLMs in predictions, to investigate their posterior and predictive distributions.

Table 1: Mean squared errors of coefficients ( $\times 10^4$ ) and forecasting ( $\times 10^3$ ) for  $t \geq 25$ .

No.	Model	Prior	Baseline	$\theta_{1t}$	$\theta_{2t}$	$\theta_{3t}$	$\theta_{4t}$	$\theta_{5:12,t}$	$y_{t+1}$
$\mathcal{M}_1$	DFL	i	0	247.62	138.08	199.21	189.29	0.01	265.04
$\mathcal{M}_2$		ii	0	245.54	134.27	194.23	187.22	0.18	257.91
$\mathcal{M}_3$		iii	0	252.71	130.82	191.44	187.08	0.60	254.93
$\mathcal{M}_4$		i	$\mu_i$	278.41	149.56	217.83	226.50	20.44	452.52
$\mathcal{M}_5$		ii	$\mu_i$	289.49	149.61	211.70	219.44	19.24	322.30
$\mathcal{M}_6$		iii	$\mu_i$	297.43	142.13	213.61	210.15	17.46	297.23
$\mathcal{M}_7$	DE	i	0	314.99	129.05	201.44	219.71	14.41	277.82
$\mathcal{M}_8$		ii	0	284.58	132.69	203.31	222.69	12.75	279.09
$\mathcal{M}_9$		iii	0	279.48	136.89	196.58	220.02	9.88	274.49
$\mathcal{M}_{10}$		i	$\mu_i$	338.60	129.01	202.09	218.18	18.00	299.67
$\mathcal{M}_{11}$		ii	$\mu_i$	345.92	124.20	197.58	216.68	18.33	302.93
$\mathcal{M}_{12}$		iii	$\mu_i$	340.67	128.66	203.42	216.80	17.98	302.72

In the estimation of dynamic coefficients, the third predictor is of the special interest for its dynamic significance. The posterior of  $\theta_{3t}$  computed by model  $\mathcal{M}_3$  is shown in Figure 6 with its true value, the posterior mean of the latent count  $n_{3t}$ , and the posterior probability of positive count  $Pr[n_{3t} > 0|y_{1:T}]$ . In addition to conforming the successful posterior analysis in the top figure, we can also observe in the middle and bottom figures that the latent count is more likely to be positive in the period when the predictor is inactive. This result is easily expected from the structure of the augmented model; if the positive count is sampled, then we additionally have the synthetic observation, whose information helps to shrink the state variable to zero in the posterior. This clear correspondence between the sparsity in state variables and the values of latent counts implies the potential interpretation of the posterior of  $n_{it}$  as the indicator of “insignificance” of state variables. This point is further examined in the next subsection through the application to the real macroeconomic dataset.

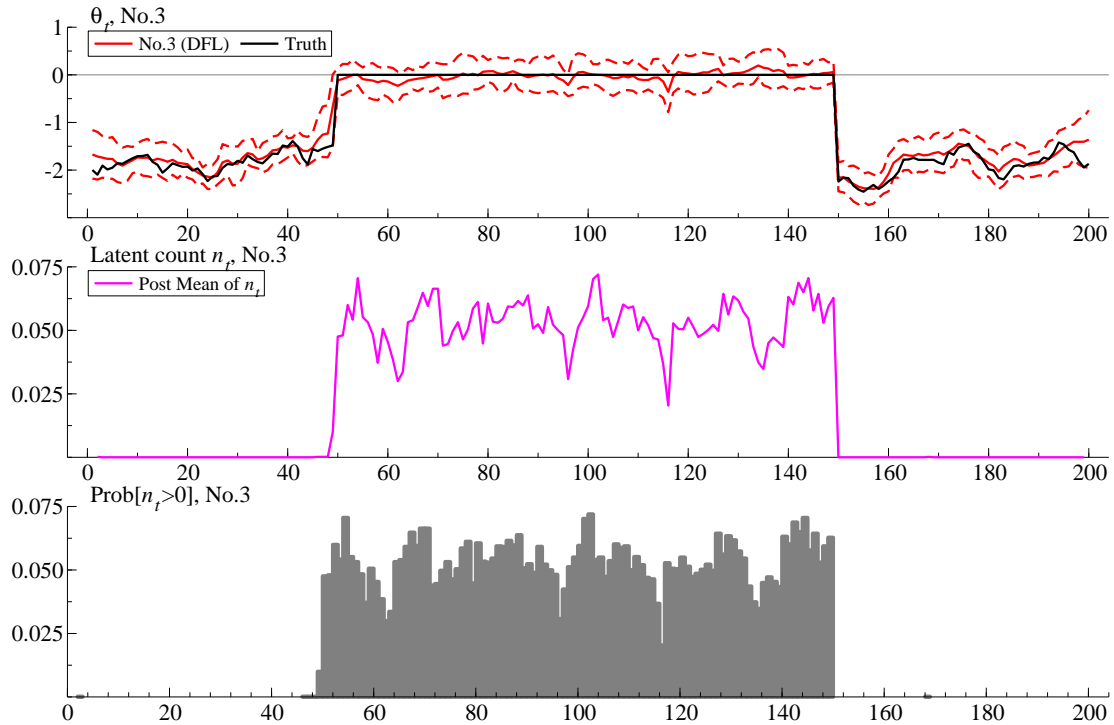


Figure 6: Top: the posterior means and 95% credible intervals of  $\theta_{3t}$  with Model 1 (red), compared with the true values (black). Middle: the posterior means of latent count  $n_{3t}$  (pink). They spike up only in the period when this predictor becomes inactive in the data generating process, suggesting that this latent variable indicates the insignificance of the predictor. Bottom: the posterior probability of positive counts, i.e.,  $Pr[n_{3t} > 0]$ . In the period of interest, this probability becomes significantly higher than those in the other periods, but its value is at most 0.075.

The posteriors of  $\alpha_i$ 's are listed in Figure 7. It is clear in this figure that the values of these weights become extremely small for the active predictors, while being sufficiently large for the inactive predictors. The extremely small value of weight  $\alpha_i$  indicates that the first penalty, or the shrinkage effect to zero, is almost negligible. In contrast, the large weight forces the model to shrink the state variable to zero more aggressively, which is the appropriate treatment of inactive predictors. The posterior densities of weight parameters for those predictors overlap their priors. This result is anticipated from the conditional distributions in Section 4.2; the contribution from the likelihood diminishes as  $\theta_{it} \approx 0$  for many  $t$ .

Figure 8a and 8b show the superimposed posterior trajectories of the state variables,  $\theta_{1t}$  and  $\theta_{5t}$ , of the

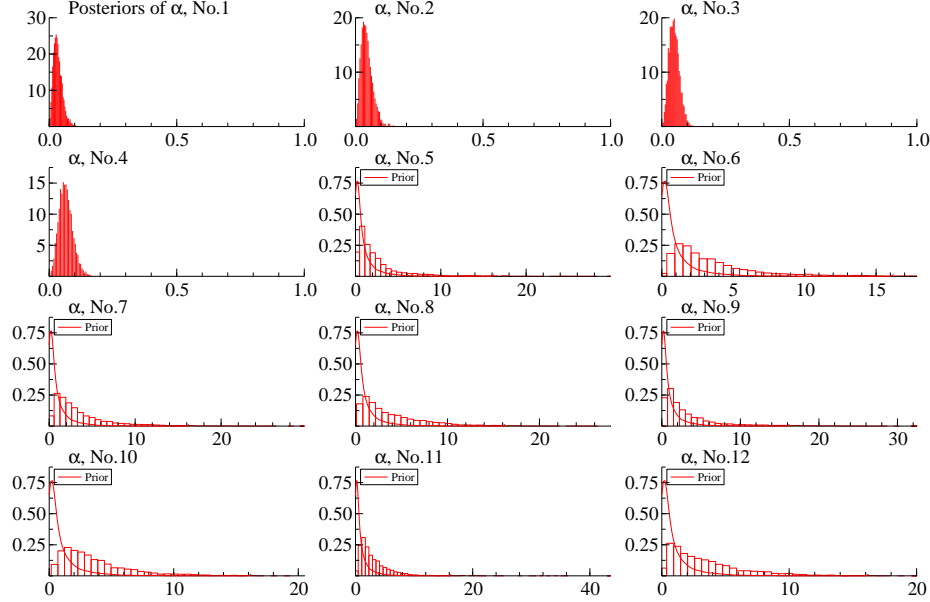


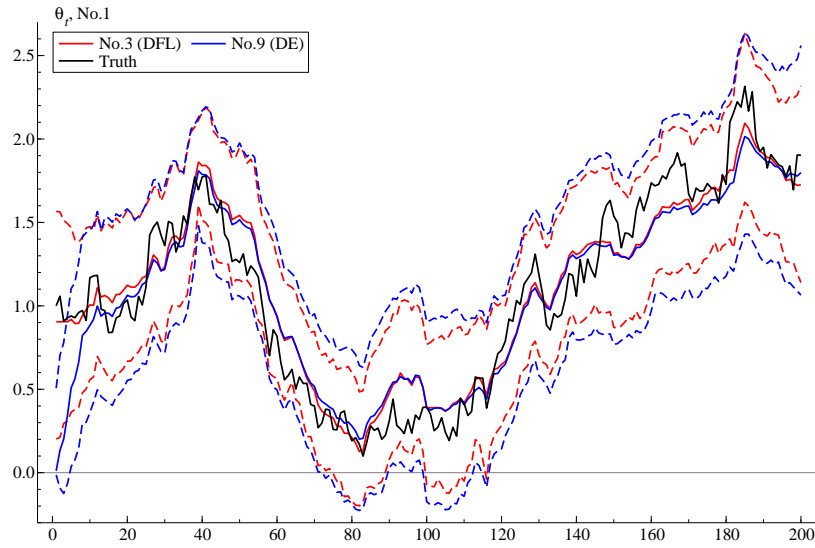
Figure 7: The posteriors of weight parameters  $\alpha_i$  for  $i \in 1 : 12$ . For the four active predictors, the value of  $\alpha_i$  is extremely small, concluding that the DFL priors for these coefficients are almost equivalent to the DE priors. For the inactive predictors, the weights can take larger values as well. In fact, the posteriors are almost the same as the priors (drawn by the solid lines).

DFL-DLM  $\mathcal{M}_3$  and DE-DLM  $\mathcal{M}_9$ . For the active predictor, as seen in the example of  $\theta_{1t}$ , the posterior mean and 95% credible intervals almost overlap all the time. This result is consistent with our observation in Figure 7 that the posterior of weight  $\alpha_i$  concentrates around small values and the DFL prior reduces to the DE prior. In contrast, the difference of the two models is clear in the uncertainty of state variables for the inactive predictors. The large weight on the first penalty induces the strong shrinkage to zero, shrinking the posterior locations to zero and narrowing the credible intervals. This shrinkage effect is escalated in  $\mathcal{M}_1$ , where the prior of  $\rho_i$  is  $Be(1, 2)$  and the posterior of state variable is almost degenerated at zero. Consequently, those noise predictors do not contribute to the entire posterior and the predictive analysis, as if they were excluded from the model.

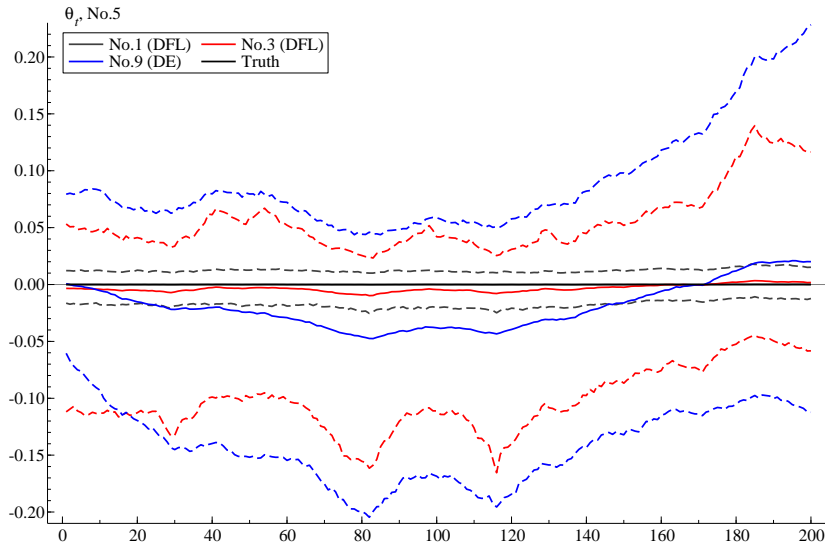
The twelve models are repeatedly estimated by the MCMC method in the sequential way, starting at time  $t = 25$ , to provide the one-step ahead forecast distributions. As seen in Table 1, the predictions by the DFL-DLMs are successful in the MSEs. However, the DFL-DLMs are shown to improve not only the accuracy of point estimation, but also the uncertainty quantification. Figure 9a and 9b show the predictive means and 95% credible intervals of  $\mathcal{M}_3$  and  $\mathcal{M}_9$  with the actual observations. The reduced predictive uncertainty is visually clear; as confirmed in Figure 7, the additional shrinkage effects are strong for the noise predictors in the DFL-DLM, which is considered to contribute to this result. The DFL-DLM is still able to cover the actual observation in its narrowed credible intervals successfully.

## 5.2 Macroeconomic data and latent threshold models

The posterior plot of latent counts  $n_{it}$ 's in Figure 6 suggests the potential use of this quantity as the indicator of (in)significance of coefficients. In this section, we further examine this aspect of the DFL prior through the comparison with the latent threshold models (LTMs), that are the more formal approach to the dynamic variable selection (e.g., Nakajima and West 2013b, 2015). The LTMs explicitly distinguish

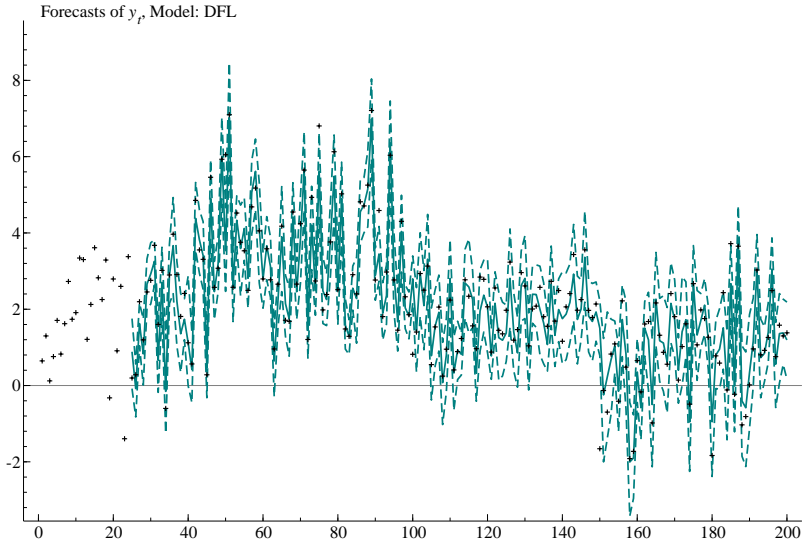


(a) The posteriors of  $\theta_{1t}$

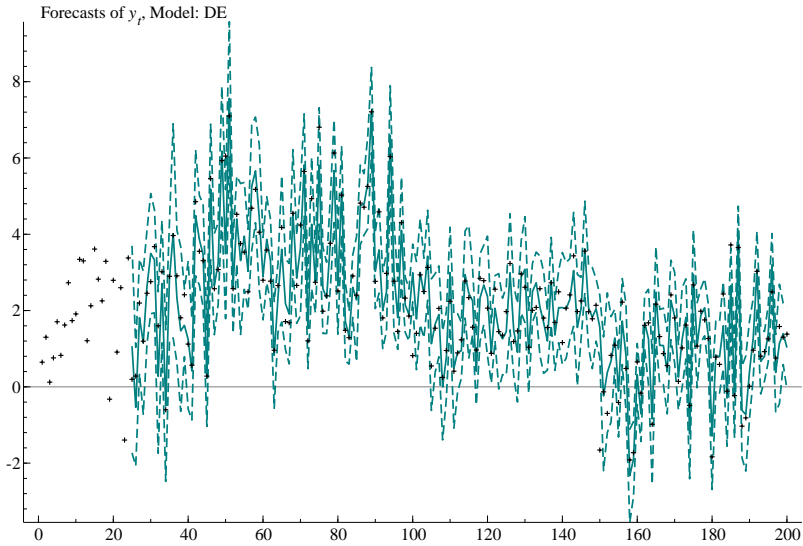


(b) The posteriors of  $\theta_{5t}$

Figure 8: Left: the posterior means and 95% credible intervals of  $\theta_{1t}$  of the DFL-DLM  $\mathcal{M}_3$  (red) and the DE-DLM  $\mathcal{M}_9$  (blue) with true values (black). The two posteriors are almost identical after  $t \geq 25$  both in the locations and uncertainty quantification. This is because of the small  $\alpha_1$  observed in Figure 7, with which the DFL prior is approximately the DE prior. Left: the same posterior plots for  $\theta_{5t}$ . For the inactive predictors, including this example, the posterior of the DFL-DLM concentrates around zero over time. This is also due to  $\alpha_i$ , that is large now and induces the additional shrinkage to zero at each time point. In another DFL-DLM  $\mathcal{M}_1$ , the posterior is almost degenerate at zero for its strong shrinkage effect to zero assumed in the prior.



(a) Forecasting by Model no.3 (DFL)



(b) Forecasting by Model no.9 (DE)

Figure 9: Left: The means and 95% credible intervals of the one-step ahead forecast distributions  $p(y_{t+1}|y_{1:t})$  for the DFL-DLM  $\mathcal{M}_3$ , Right: DE-DLM  $\mathcal{M}_9$ . Both models are able to predict the next observation reasonably, but the DFL-DLM is more successful in uncertainty quantification for its narrower credible intervals. The accuracy of point forecasting in these models can be seen in Table 1.

the latent and realized state variables,  $\theta_{it}^*$  and  $\theta_{it}$  for  $i$ -th coefficient, and connect them by the indicator function as,

$$\theta_{it} = s_{it}\theta_{it}^*, \quad \text{and} \quad s_{it} = 1[|\theta_{it}^*| > d_i], \quad (21)$$

where latent state variable  $\theta_{it}^*$  follows a Gaussian AR(1) process and  $d_i$  is some positive, non-dynamic threshold. The probability that this coefficient is significant at time  $t$  is parametrized by  $Pr[s_t = 1]$  and can be computed explicitly in the posterior analysis. Despite this interpretable model specification, as is generally true for any model of variable selection, the posterior analysis of the LTMs by MCMC methods is computationally costly, both in coding and computational time.

The example of the LTM and its application to the analysis of the US macroeconomic variables are taken from Nakajima and West (2013a). The vector of the inflation, unemployment and nominal interest rates is denoted by  $y_t$  and observed quarterly between 1977 and 2007. The base model is the time-varying vector autoregressive model with order 3, the likelihood of which is

$$y_t = c_t + B_{1t}y_{t-1} + B_{2t}y_{t-2} + B_{3t}y_{t-3} + N(0, \Omega_t^{-1}), \quad \Omega_t = (I - A_t)\Lambda_t(I - A_t)',$$

where  $\Lambda_t$  is the diagonal matrix of log-Gaussian stochastic volatilities and  $A_t$  is the lower-triangular matrix with diagonal zeros. Each entry of  $c_t$ ,  $B_{1:3,t}$  and  $A_t$  follows the Gaussian, stationary AR(1) process with latent threshold in (21). The parameters of interest are  $B_{1:3,t}$  and  $A_t$ , that determine the lagged/simultaneous correlation between variables. The graphical, conditional dependence structure of the three macroeconomic variables captured by  $A_t$ , or  $\Omega_t$ , is of great importance in the macroeconomic studies. For the details of the model, prior and computation, see Nakajima and West (2013a).

In this study, our interest is in whether the time-varying vector autoregressive models with the DFL prior can achieve the same objective of having the sparse structure in  $B_{1:3,t}$  and  $A_t$ . The DFL prior is used for  $c_t$ ,  $B_{1:3,t}$  and  $A_t$  to compute the posterior of the latent counts  $n_{it}$ , or  $Pr[n_{it} > 0 | y_{1:T}]$ , that are expected to approximate the posterior exclusion probability  $Pr[s_{it} = 1 | y_{1:T}]$  of the LTM. Because the prior processes for  $c_t$  and  $B_{1:3,t}$  are more persistent than those for  $A_t$  in the LTM, we adjust the hyperparameters in the DFL prior as  $\beta_i \sim Ga(4, 0.1)$  for the former and  $Ga(2, 0.1)$  for the latter. Similarly, because we have more parameters in the regression on the lagged terms, we set the DFL prior as  $\rho_i \sim Be(1, 2)$  for  $c_t$  and  $B_{1:3,t}$  and  $\rho_i \sim Be(1, 10)$  for  $A_t$ . The posteriors are computed based on 50,000 iterations in the Gibbs sampler after 5,000 burn-in. The chain is set relatively long, due to the slow convergence of volatility-related parameters generated by the single-move sampler.

For the nine state variables in  $B_{1t}$ , the posterior exclusion probabilities for the LTM and the posterior probability of positive counts for the DFL-DLM are displayed in Figure 10a and 10b, respectively. While the LTM shows its volatile decisions on inclusion/exclusion of predictors, the DFL-DLM consistently makes the diagonal elements active. These diagonal entries correspond with the autoregressive terms, realizing the autocorrelation of the three series. For some off-diagonal entries, both models agree on excluding the predictors (e.g., (1, 3)-entry). In the DFL-DLM, the probability of  $n_{it} > 0$  is never as high as 1, but at most 0.4. Compared with the posteriors of the diagonal entries of  $B_{1t}$ , it is empirically judged that the value of 0.4 is large enough to induce the strong shrinkage effect on the corresponding predictors that are not active. This point can be double-checked in the estimates of coefficients shown in Figure 11a and 11b, where we observe the DFL-DLM has larger estimates of the diagonal coefficients, while shrinking all the other parameters to zero.

The same outputs of the posterior analysis for  $A_t$  are shown in in Figure 12a and 12b. In Figure 12a and 12b, respectively. Although both models deny the activeness of simultaneous correlations, in Figure 12a, the LTM leaves 40% probability of including the third parameter, i.e., the simultaneous regression of the interest rate on the unemployment rate. The posterior probabilities of positive counts in the DFL are much smaller than 0.4 in Figure 12b, yet the estimates of coefficients seem strongly shrunk to zero. The estimates of the latent coefficients in the LTMs seemingly deviate from zero, but note that these

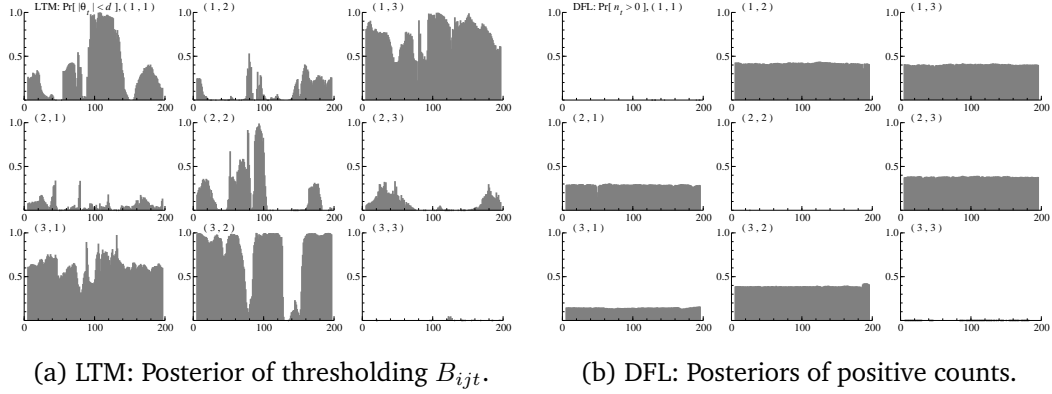


Figure 10: Left: the posterior probability of the LTM that  $|\theta_{ijt} < d_{ij}|$ , where  $\theta_{ijt}$  is the latent version of the  $(i, j)$ -entry of  $B_{1t}$  and  $d_{ij}$  is the corresponding threshold. Right: the posterior probability of observing positive latent counts for each of  $B_{1t}$  in the DFL-DLM. The former is volatile over time, while the latter is stable. The diagonal elements are the autoregressive effects, all of which are significant in the DFL-DLM. For the off-diagonal elements, the results of the two models coincide in some cases (e.g.,  $(1, 3)$ -entry).

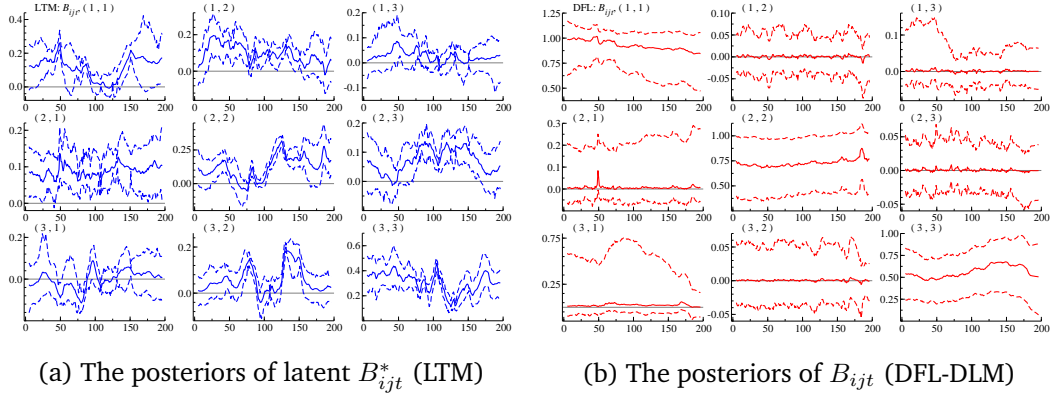


Figure 11: Left: the posteriors of latent state variables in  $B_{1t}$  for the LTM, Right: the posteriors of the state variables in  $B_{1t}$  in the DFL-DLM. Note that the latent state variables in the LTM are not identified when they are thresholded. The diagonal elements in the DFL-DLM are larger than those of the LTM, while the other off-diagonal entries are all shrunk to zero in the DFL-DLM.

parameters are not identified when they are thresholded. From either model, we may conclude that the information on the graphical structure in this dataset is limited.

Overall, in contrast to the study of simulated data, the posterior probabilities of positive counts are less dynamic, both for  $B_{1t}$  and  $A_t$ . It is concluded that the dynamic change of the strength of signals in the real data is not as clear as in the simulated data that we artificially create for the illustration. One can emphasize the dynamic significance in the posteriors by choosing another set of hyperparameters that makes the DLF prior more informative, but the overall trend of posterior results, such as the significance of the diagonal elements of  $B_{1t}$ , remains unchanged.



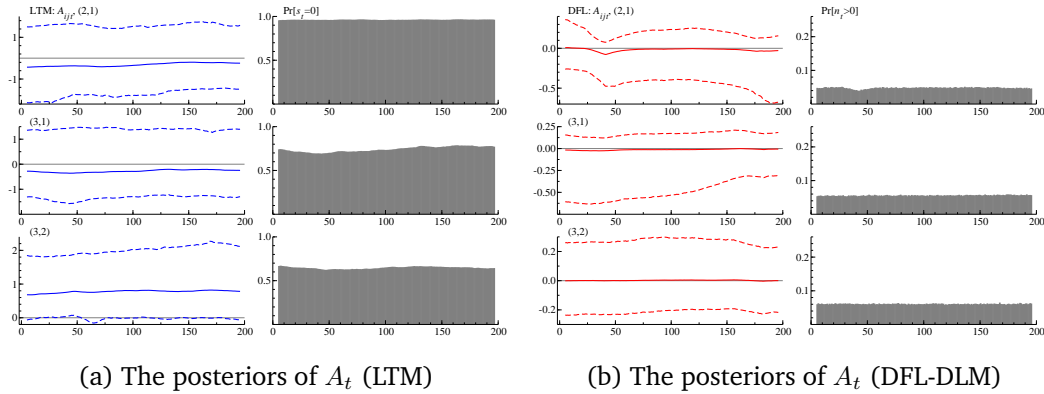


Figure 12: Left: the posteriors of latent state variables and their exclusion probabilities for the lower-triangular elements in  $A_{it}$  in the LTM, Right: the posteriors of the state variables and positive counts for  $A_t$  in the DFL-DLM. In both results, the simultaneous regressors are all insignificant and it is difficult to find out the graphical structure in this dataset. While the DFL-DLM shrink all these parameters strongly to zero in all time, the LTM has some posterior uncertainty on the exclusion of those predictors, especially for the third parameter, i.e., the simultaneous regression coefficient between the unemployment and interest rates.

## 6 Concluding Remark

This research on the DFL process is the formal Bayesian attempt at the introduction of the multiple, conflicting shrinkage effects. The additional shrinkage newly introduced in the DLF process is separated from the existing shrinkage on dynamics and comprises the synthetic likelihood, with which the model becomes the CDLM and allows the posterior computation by FFBS. The latent integer-valued variable serves as the indicator of signals from that predictor and the DFL-DLM behaves as the dynamic variable selection models.

The research of this type can be further developed in several directions. For example, the prior density that consists of three and more penalty functions is of great interest, not only in time series analysis and the fuse LASSO models, but also in the spatial models that account for the geographical relationships by the multiple shrinkage effects. Another promising future research is to consider the different loss functions and the combination of them, e.g., Example 2 (Bayesian elastic net) and Example 4 (horseshoe prior) in Section 2. If those priors are also proven to have the normalizing functions that are analytically available and augmented to the CDLM, the posterior computations are greatly simplified in the similar way to the DFL prior. Otherwise, one can start from defining the mixture of DLMs with different synthetic likelihood and prior and, retrospectively, transforming the CDLM back to the prior process. Either research will contribute to the development of the more flexible dynamic models.

## References

- Andrews, D. F. and Mallows, C. L. (1974). “Scale mixtures of normal distributions.” *Journal of the Royal Statistical Society (Series B: Methodological)*, 36: 99–102.
- Belmonte, M. A., Koop, G., and Korobilis, D. (2014). “Hierarchical shrinkage in time-varying parameter models.” *Journal of Forecasting*, 33(1): 80–94.

- Betancourt, B., Rodríguez, A., and Boyd, N. (2017). “Bayesian Fused Lasso regression for dynamic binary networks.” *Journal of Computational and Graphical Statistics*, 26(4): 840–850.
- Bitto, A. and Frühwirth-Schnatter, S. (2019). “Achieving shrinkage in a time-varying parameter model framework.” *Journal of Econometrics*, 210(1): 75–97.
- Carvalho, C. M., Polson, N. G., and Scott, J. G. (2009). “Handling Sparsity via the Horseshoe.” In *AISTATS*, volume 5, 73–80.
- (2010). “The horseshoe estimator for sparse signals.” *Biometrika*, 97(2): 465–480.
- Devroye, L. (2014). “Random variate generation for the generalized inverse Gaussian distribution.” *Statistics and Computing*, 24(2): 239–246.
- Doornik, J. A. (2007). *Object-Oriented Matrix Programming Using Ox, 3rd ed.*. London: Timberlake Consultants Press and Oxford, 3rd edition.
- Frühwirth-Schnatter, S. and Wagner, H. (2010). “Stochastic model specification search for Gaussian and partial non-Gaussian state space models.” *Journal of Econometrics*, 154(1): 85–100.
- Gelman, A. (2006). “Prior distributions for variance parameters in hierarchical models (comment on article by Browne and Draper).” *Bayesian analysis*, 1(3): 515–534.
- Gruber, L. and West, M. (2016). “GPU-accelerated Bayesian learning in simultaneous graphical dynamic linear models.” *Bayesian Analysis*, 11(1): 125–149.
- Hans, C. (2009). “Bayesian lasso regression.” *Biometrika*, 96(4): 835–845.
- (2011). “Elastic net regression modeling with the orthant normal prior.” *Journal of the American Statistical Association*, 106(496): 1383–1393.
- Irie, K. and West, M. (2019). “Bayesian Emulation for Multi-Step Optimization in Decision Problems.” *Bayesian Analysis*, 14(1): 137–160.
- Kalli, M. and Griffin, J. E. (2014). “Time-varying sparsity in dynamic regression models.” *Journal of Econometrics*, 178(2): 779–793.
- Kim, S., Shephard, N., and Chib, S. (1998). “Stochastic volatility: likelihood inference and comparison with ARCH models.” *The review of economic studies*, 65(3): 361–393.
- Kolm, P. N. and Ritter, G. (2015). “Multiperiod portfolio selection and Bayesian dynamic models.” *Risk*, 28: 50–54.
- Kowal, D. R., Matteson, D. S., and Ruppert, D. (2019). “Dynamic shrinkage processes.” *Journal of Royal Statistical Society*, forthcoming.
- Kyung, M., Gill, J., Ghosh, M., Casella, G., et al. (2010). “Penalized regression, standard errors, and Bayesian lassos.” *Bayesian Analysis*, 5(2): 369–411.
- Müller, P. (1999). “Simulation based optimal design.” In Bernardo, J. M., Berger, J. O., Dawid, A. P., and Smith, A. F. M. (eds.), *Bayesian Statistics 6*, 459–474. Oxford University Press.
- Nakajima, J. and West, M. (2013a). “Bayesian analysis of latent threshold dynamic models.” *Journal of Business and Economic Statistics*, 31: 151–164.

- (2013b). “Bayesian dynamic factor models: Latent threshold approach.” *Journal of Financial Econometrics*, 11: 116–153.
- (2015). “Dynamic network signal processing using latent threshold models.” *Digital Signal Processing*, 47: 6–15.
- Omori, Y., Chib, S., Shephard, N., and Nakajima, J. (2007). “Stochastic volatility with leverage: Fast and efficient likelihood inference.” *Journal of Econometrics*, 140(2): 425–449.
- Park, T. and Casella, G. (2008). “The Bayesian lasso.” *Journal of the American Statistical Association*, 103: 681–686.
- Polson, N. G., Scott, J. G., and Windle, J. (2014). “The bayesian bridge.” *Journal of the Royal Statistical Society: Series B (Statistical Methodology)*, 76(4): 713–733.
- Uribe, P. V. and Lopes, H. F. (2017). “Dynamic sparsity on dynamic regression models.” *Manuscript, available at <http://hedibert.org/wpcontent/uploads/2018/06/uribe-lopes-Sep2017.pdf>*.
- Van Dyk, D. A. and Park, T. (2008). “Partially collapsed Gibbs samplers: Theory and methods.” *Journal of the American Statistical Association*, 103(482): 790–796.
- West, M. (1984). “Outlier models and prior distributions in Bayesian linear regression.” *Journal of the Royal Statistical Society (Series B: Methodological)*, 46: 431–439.
- (1987). “On scale mixtures of normal distributions.” *Biometrika*, 74: 646–648.
- West, M. and Harrison, P. J. (1997). *Bayesian Forecasting and Dynamic Models*. Springer Verlag, 2nd edition.
- Zhao, Z. Y., Xie, M., and West, M. (2016). “Dynamic dependence networks: Financial time series forecasting and portfolio decisions.” *Applied Stochastic Models in Business and Industry*, 32(3): 311–332.

## Appendix

### Computation for Proposition 3.5

The joint density of  $(w, z) = (\tau_1/(\tau_1 + \tau_2), \tau_1 + \tau_2)$  is

$$\begin{aligned} q(w, z) &= \frac{N(x'|0, z)}{h(x')} Ga(wz|1, a^2/2) Ga((1-w)z|1, b^2/2)z \\ &= \frac{a^2b^2}{4\sqrt{2\pi}h(x')} z^{3/2-1} \exp \left\{ -\frac{wa^2 + (1-w)b^2}{2}z - \frac{(x')^2}{2z} \right\} \end{aligned}$$

where we read off the conditional/marginal densities,  $q(z|w)q(w)$  or  $q(w|z)q(z)$ . In the former, given  $w$ , we see  $z|w \sim GIG(3/2, wa^2 + (1-w)b^2, (x')^2)$ . Marginalizing  $z$  out, we have

$$\begin{aligned} q(w) &= \frac{a^2b^2}{4\sqrt{2\pi}h(x')} \frac{2K_{3/2}(\sqrt{(wa^2 + (1-w)b^2})(x')^2)}{(wa^2 + (1-w)b^2/(x')^2)^{3/4}} \\ &= \frac{a^2b^2}{4h(x')} e^{-|x'|\sqrt{wa^2+(1-w)b^2}} \frac{|x'|}{wa^2 + (1-w)b^2} \left( 1 + \frac{1}{|x'|\sqrt{wa^2 + (1-w)b^2}} \right) \end{aligned}$$

which proves Proposition 3.5. Sampling  $w$  from this marginal distribution is not straightforward. The simplest method of sampling is to use the discrete prior on the points in  $(0, 1)$  because the density can be evaluated at each point. However, we pursue the more efficient sampling by the inverse method by utilizing the functional form of the density. Consider the change of variable where  $y = |x'|\sqrt{wa^2 + (1-w)b^2}$ ,  $y \in (a|x'|, b|x'|)$  and  $dw = 2y^{1/2}dy/(b^2 - a^2)|x'|$ , to obtain the density in equation (16). The integral of this density is computed by integral by parts and becomes the form in (17).

Sampling from  $p(x|x')$ .

1. Sample  $u \sim U(0, 1)$ .
2. Given  $u$ , set  $y = Q^{-1}(u)$ .  
Recover  $w$  by  $w = (b^2 - y^2/|x'|^2)/(b^2 - a^2)$ .
3. Given  $w$ , sample  $z \sim GIG(3/2, wa^2 + (1-w)b^2, (x')^2)$ .
4. Given  $(w, z)$ , sample  $x \sim N(wx', w(1-w)z)$ .

---

For the computation of  $Q^{-1}$ , the simple Newton method can be applied and satisfactorily efficient. To compute  $y = Q^{-1}(u)$  for given  $u$ , one must solve the equality

$$u = \frac{be^{-a|x'|} - ab|x'|y^{-1}e^{-y}}{be^{-a|x'|} - ae^{-b|x'|}} \quad \text{or, equivalently,} \quad y^{-1}e^{-y} = y_0 = \frac{be^{-a|x'|} - u\{be^{-a|x'|} - ae^{-b|x'|}\}}{ab|x'|}$$

in  $y$ . Further, by taking  $z = \log(y) \in (\log(a) + \log|x'|, \log(b) + \log|x'|)$  and  $z_0 = \log(y_0)$ , we have

$$g(z) = z + e^z + z_0 = 0.$$

The Newton method for solving this equation is defined by the update rule of the sequence  $\{z_n\}$  as

$$z_{n+1} = z_n - \frac{g(z_n)}{g'(z_n)} = z_n - \frac{z_n + e^{z_n} + z_0}{1 + e^{z_n}}$$

until the increment is less than the tolerance level.

The other way of decomposition,  $q(w|z)q(z)$ , is useful, for example, in deriving the expectation  $E[w|x']$ . The conditional density of  $(w|z)$  is  $q(w|z) \propto e^{(b^2-a^2)zw/2}$ , whose normalizing constant is

$$\int_0^1 e^{(b^2-a^2)zw/2} dw = \frac{2}{(b^2-a^2)z} \left\{ e^{(b^2-a^2)z/2} - 1 \right\}$$

Next, the marginal of  $z$  is

$$q(z) = \frac{a^2 b^2}{2\sqrt{2\pi}(b^2-a^2)h(x')} z^{-1/2} \exp\left\{-\frac{(x')^2}{2z}\right\} \left\{ e^{-a^2 z/2} - e^{-b^2 z/2} \right\}$$

This is the *difference* of two GIG densities, not the mixture, hence not suitable for the random number generation. This form is rather useful in computing the moments.

We derive  $E[w|x']$  in the closed form as shown in Proposition 3.5. First, compute the following integral, by using the integral by parts,

$$\begin{aligned} \int_0^1 w e^{(b^2-a^2)zw/2} dw &= \left[ w \frac{2}{(b^2-a^2)z} e^{(b^2-a^2)zw/2} \right]_0^1 - \frac{2}{(b^2-a^2)z} \int_0^1 e^{(b^2-a^2)zw/2} dw \\ &= \frac{2}{(b^2-a^2)z} \left[ e^{(b^2-a^2)z/2} - \frac{2}{(b^2-a^2)z} \left\{ e^{(b^2-a^2)z/2} - 1 \right\} \right] \end{aligned}$$

Denote the normalizing constant of  $GIG(p, \alpha, \beta)$  by  $G(p, \alpha, \beta)$ . Then,

$$\begin{aligned} E[w|x'] &= \int_0^\infty \int_0^1 w q(z, w) dw dz \\ &= \frac{a^2 b^2}{2\sqrt{2\pi}(b^2-a^2)h(x')} \left[ G(1/2, a^2, (x')^2) - \frac{2}{(b^2-a^2)} \left\{ G(-1/2, a^2, (x')^2) - G(1/2, b^2, (x')^2) \right\} \right] \\ &= \frac{a^2 b^2}{2(b^2-a^2)} \left[ \frac{1}{a} e^{-a|x'|} - \frac{2}{(b^2-a^2)|x'|} \left\{ e^{-a|x'|} - e^{-b|x'|} \right\} \right] \end{aligned}$$

which is further simplified by substituting  $h(x')$  and shows the expression of Proposition 3.5.

## Sampling of observational variance

The scale-free DLM with the DFL prior has the CDLM form as follows;

$$\begin{aligned} y_t | \theta_t, V &\sim N(F_t' \theta_t, V) \\ z_{it} | \theta_t, V &\sim N(\theta_{it}, V \lambda_{n,it}), \quad \text{if } n_{it} > 0 \\ z_{iT} | \theta_T, V &\sim N(\theta_{iT}, V \lambda_{a,it}) \\ \theta_{i1} | V &\sim N(\mu_i, V \lambda_{a,i1}) \\ \theta_{it} | \theta_{i,t-1}, V &\sim N(\theta_{b,t-1}, V \lambda_{b,it}) \end{aligned} \tag{22}$$

where  $z_{it} = \mu_i$  for all  $t$  and  $i$ . The MCMC algorithm is modified by replacing the sampling of state variables as follows;

---

Gibbs sampler for scale-free models: replace Step 1 of the algorithm in Section 4.1 by the following.

1. Sampling  $\theta_{1:p,1:T}$  and  $V$ .

(i) Forward filtering.

For the DLM in equation (22), implement the forward filtering to compute the one-step ahead predictive density; for  $y_t^* = (y_t, z_t)'$ , where  $z_t$  is the collection of observed  $z_{1:p,t}$  ( $z_{it} \in z_t$  if  $n_{it} > 0$ ),

$$p(y_t^* | y_{1:t-1}^*) = N(y_t^* | f_t, VQ_t^*)$$

(ii) Sampling of  $V$ .

Generate  $V$  from its posterior  $Ga(n_T/2, n_T S_T/2)$ , where the sufficient statistics can be computed by

$$n_t = n_{t-1} + 1, \quad S_t = n_{t-1} S_{t-1} + (y_t^* - f_t)' (Q_t^*)^{-1} (y_t^* - f_t)$$

(iii) Sampling of  $(\theta_{1:p,1:T} | V)$  Given  $V$ , implement the forward filtering and backward sampling for the model in equation (22) to generate  $\theta_{1:p,1:T}$ .

---

The sampling of the other parameters remain the same for the scaled state variable  $\theta_{it}/\sqrt{V}$ .

This approach to the scale-free models can be applied to the case of stochastic volatility; replace  $V$  in the conditional model by  $V_t$  and model  $V_t^{-1}$  by the gamma-scale beta evolution sequentially. The FFBS for  $V_t$  can be derived in a similar way. For more details, see (West and Harrison, 1997), Chapter 10.8.